

Non-reversible Parallel Tempering for Deep Posterior Approximation

Wei Deng^{*1, 2}, Qian Zhang^{*1}, Qi Feng^{*3}, Faming Liang¹, Guang Lin¹

¹ Purdue University ² Morgan Stanley ³ University of Michigan
weideng056@gmail.com guanglin@purdue.edu

Abstract

Parallel tempering (PT), also known as replica exchange, is the go-to workhorse for simulations of multi-modal distributions. The key to the success of PT is to adopt efficient swap schemes. The popular deterministic even-odd (DEO) scheme exploits the non-reversibility property and has successfully reduced the communication cost from $O(P^2)$ to $O(P)$ given sufficiently many P chains. However, such an innovation largely disappears in big data due to the limited chains and few bias-corrected swaps. To handle this issue, we generalize the DEO scheme to promote non-reversibility and propose a few solutions to tackle the underlying bias caused by the geometric stopping time. Notably, in big data scenarios, we obtain an appealing communication cost $O(P \log P)$ based on the optimal window size. In addition, we also adopt stochastic gradient descent (SGD) with large and constant learning rates as exploration kernels. Such a user-friendly nature enables us to conduct approximation tasks for complex posteriors without much tuning costs.

Introduction

Langevin diffusion is a standard sampling algorithm that follows a stochastic differential equation

$$d\beta_t = -\nabla U(\beta_t)dt + \sqrt{2\tau}d\mathbf{W}_t,$$

where $\beta_t \in \mathbb{R}^d$, $U(\cdot)$ is the energy function $U(\cdot)$, $\mathbf{W}_t \in \mathbb{R}^d$ is a Brownian motion, and τ is the temperature. The diffusion process converges to a stationary distribution $\pi(\beta) \propto e^{-\frac{U(\beta)}{\tau}}$ and setting $\tau = 1$ yields a Bayesian posterior. A convex $U(\cdot)$ leads to a rapid convergence (Durmus and Moulines 2016; Dalalyan 2017); however, a non-convex $U(\cdot)$ inevitably slows down the mixing rate (Raginsky, Rakhlin, and Telgarsky 2017; Liu and Wang 2016; Deng et al. 2022; Deng, Lin, and Liang 2022). To accelerate simulations, replica exchange Langevin diffusion (reLD) proposes to include a high-temperature particle $\beta_t^{(P)}$, where $P \in \mathbb{N}^+ \setminus \{1\}$, for *exploration*. Meanwhile, a low-temperature particle $\beta_t^{(1)}$ is presented

for *exploitation*:

$$\begin{aligned} d\beta_t^{(P)} &= -\nabla U(\beta_t^{(P)})dt + \sqrt{2\tau^{(P)}}d\mathbf{W}_t^{(P)} \\ d\beta_t^{(1)} &= -\nabla U(\beta_t^{(1)})dt + \sqrt{2\tau^{(1)}}d\mathbf{W}_t^{(1)}, \end{aligned} \quad (1)$$

where $\tau^{(P)} > \tau^{(1)}$ and $\mathbf{W}_t^{(P)}$ is independent of $\mathbf{W}_t^{(1)}$. To promote more explorations for the low-temperature particle, the particles at the position $(\beta^{(1)}, \beta^{(P)}) \in \mathbb{R}^{2d}$ swap with a probability $aS(\beta^{(1)}, \beta^{(P)})$, where

$$S(\beta^{(1)}, \beta^{(P)}) = 1 \wedge e^{\left(\frac{1}{\tau^{(1)}} - \frac{1}{\tau^{(P)}}\right)(U(\beta^{(1)}) - U(\beta^{(P)}))}, \quad (2)$$

and $a \in (0, \infty)$ is the swap intensity. To be specific, the conditional swap rate at time t follows that

$$\begin{aligned} \mathbb{P}(\beta_{t+dt} = (\beta^{(P)}, \beta^{(1)}) | \beta_t = (\beta^{(1)}, \beta^{(P)})) \\ = aS(\beta^{(1)}, \beta^{(P)})dt. \end{aligned}$$

In the longtime limit, the Markov jump process converges to the joint distribution $\pi(\beta^{(1)}, \beta^{(P)}) \propto e^{-\frac{U(\beta^{(1)})}{\tau^{(1)}} - \frac{U(\beta^{(P)})}{\tau^{(P)}}$, where the marginals are denote by $\pi^{(1)}(\beta) \propto e^{-\frac{U(\beta)}{\tau^{(1)}}$ and $\pi^{(P)}(\beta) \propto e^{-\frac{U(\beta)}{\tau^{(P)}}$.

Preliminaries

Achieving sufficient explorations requires a large $\tau^{(P)}$, which leads to limited accelerations due to a *small overlap* between $\pi^{(1)}$ and $\pi^{(P)}$. To tackle this issue, one can bring in multiple particles with temperatures $(\tau^{(2)}, \dots, \tau^{(P-1)})$, where $\tau^{(1)} < \tau^{(2)} < \dots < \tau^{(P)}$, to hollow out “tunnels”. To maintain feasibility, numerous schemes are presented to select candidate pairs to attempt the swaps.

APE The all-pairs exchange (APE) attempts to swap arbitrary pair of chains (Brenner et al. 2007; Lingenheil et al. 2009), however, such a method requires a swap time (see definition in section A.5 (appendix)) of $O(P^3)$ and may not be user-friendly in practice.

ADJ In addition to swap arbitrary pairs, one can also swap *adjacent* (ADJ) pairs iteratively from $(1, 2)$, $(2, 3)$, to $(P-1, P)$ under the Metropolis rule. Despite the convenience, the *sequential nature* requires to wait for

*These authors contributed equally.

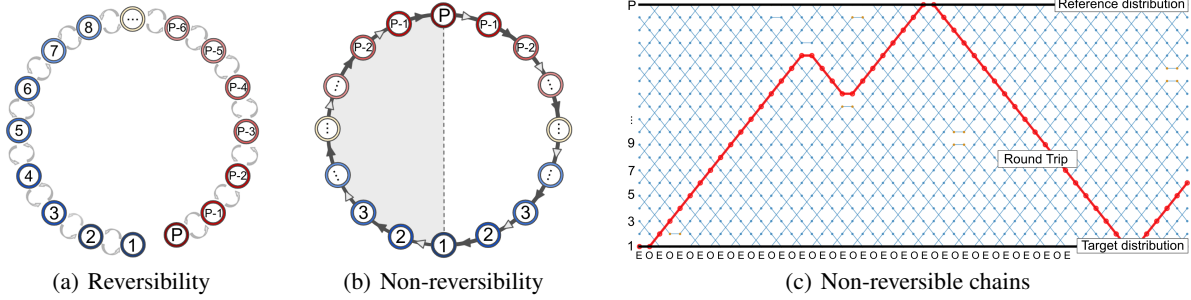


Figure 1: (Non-)Reversibility. (a): a reversible index that takes $O(P^2)$ time to communicate; (b): a linear non-reversible index moves along a periodic orbit; (c): non-reversible chains via DEO schemes.

exchange information from previous exchanges, which only works well with a small number of chains and has greatly limited its extension to a multi-core or distributed context.

SEO The stochastic even-odd (SEO) scheme first divides the adjacent pairs $\{(p-1, p) | p = 2, \dots, P\}$ into E and O , where E and O denote even and odd pairs of forms $(2p-1, 2p)$ and $(2p, 2p+1)$, respectively. Then, SEO randomly picks E or O pairs with an equal chance in each iteration to attempt the swaps. Notably, it can be conducted *simultaneously* without waiting from other chains. The scheme yields a reversible process (see Figure 1(a)), however, the gains in overcoming the sequential obstacle don't offset the $O(P^2)$ round trip time and SEO is still not effective enough.

DEO The deterministic even-odd (DEO) scheme instead attempts to swap even (E) pairs at even (E) iterations and odd (O) pairs at odd (O) iterations alternately[†] (Okabe et al. 2001). The asymmetric manner was later interpreted as a non-reversible PT (Syed et al. 2021) and an ideal index process follows a periodic orbit, as shown in Figure 1(b). With a large swap rate, Figure 1(c) shows how the scheme yields an almost straight path and a linear round trip time can be expected.

Equi-acceptance The power of PT hinges on maximizing the number of round trips, which is equivalent to minimizing $\sum_{p=1}^{P-1} \frac{1}{1-r_p}$ (Nadler and Hansmann 2007a), where r_p denotes the rejection rate for the chain pair $(p, p+1)$. Moreover, $\sum_{p=1}^{P-1} r_p$ converges to a fixed barrier Λ as $P \rightarrow \infty$ (Predescu, Predescu, and Ciobanu 2004; Syed et al. 2021). Applying Lagrange multiplies to the constrained optimization problem leads to $r_1 = r_2 = \dots = r_{P-1} := r$, where r is the *equi-rejection rate*. In general, a quadratic round trip time is required for ADJ and SEO due to the reversible indexes. By contrast, DEO only yields a *linear round trip time* in terms of P as $P \rightarrow \infty$ (Syed et al. 2021).

[†] E (O) shown in iterations means even (odd) iterations and denotes even (odd) pairs for chain indexes.

Optimal non-reversible scheme for PT

The linear round trip time is appealing for maximizing the algorithmic potential, however, such an advance only occurs given sufficiently many chains. In *non-asymptotic settings* with limited chains, a pearl of wisdom is to avoid frequent swaps (Dupuis et al. 2012) and to keep the average acceptance rate from 20% to 40% (Kone and Kofke 2005; Lingenheil et al. 2009; Atchadé, Roberts, and Rosenthal 2011). Most importantly, the acceptance rates are severely reduced in big data due to the bias-corrected swaps associated with stochastic energies (Deng et al. 2020), see details in section A.1 (appendix). As such, maintaining low rejection rates in big data becomes quite challenging and the *issue of quadratic costs* still exists.

Generalized DEO scheme

Continuing the equi-acceptance settings, we see in Figure 2(a) that the probability for the blue particle to move upward 2 steps to maintain the same momentum after a pair of even and odd iterations is $(1-r)^2$. As such, with a large equi-rejection rate r , the blue particle often makes little progress (Figure 2(b-d)). To handle this issue, the key is to propose small enough rejection rates to track the periodic orbit in Figure 1(b). Instead of pursuing excessive amount of chains, we resort to a different solution by introducing the *generalized even and odd iterations* E_W and O_W , where $W \in \mathbb{N}^+$, $E_W = \{\lfloor \frac{k}{W} \rfloor \bmod 2 = 0 | k = 1, 2, \dots, \infty\}$ and $O_W = \{\lfloor \frac{k}{W} \rfloor \bmod 2 = 1 | k = 1, 2, \dots, \infty\}$. Now, we present the generalized DEO scheme with a window size W as follows and refer to it as DEO_W :[§]

- Attempt to swap E (or O) pairs at E_W (or O_W) iterations.
- Allow *at most one* swap at E_W (or O_W) iterations.

As shown in Figure 2(e), the blue particle has a larger chance of $(1-r^2)^2$ to move upward 2 steps given $W = 2$ instead of $(1-r)^2$ when $W = 1$, although the window number is also halved. Such a trade-off inspires us to an-

[§]The generalized DEO with the optimal window size is denoted by DEO_* and will be studied in the section of Analysis of optimal window size and round trip time.

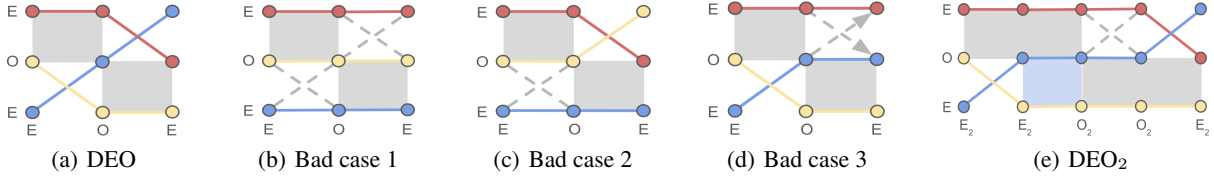


Figure 2: Illustration of DEO and DEO₂. (a): an ideal DEO scheme; (b-d): failed DEO swaps given a large r ; (e): how DEO₂ tackles the issue. The x-axis and y-axis denote (generalized) E (or O) iterations and E (or O) pairs, respectively. The dashed line denotes no swap; the gray areas are frozen to refuse swapping odd pairs at even iterations (or vice versa); the blue area freezes swap attempts.

alyze the expected round trip time based on the window of size W .

How to alleviate the bias Although allowing at most one swap introduces the geometric stopping of swaps and affects the target distribution (see section 2 of (Gerber, Shiu, and Yang 2015)), the bias can be much alleviated empirically by introducing a window-wise correction term. Moreover, it becomes rather mild when the energy estimators have a large variance. Check section C.2 (appendix) for the details. For tasks without high-accuracy demands, we propose to ignore the correction term in practice following Li et al. (2016) to facilitate the round trip analysis and promote more tractable explorations.

Analysis of round trip time

To bring sufficient interactions between the reference distribution $\pi^{(P)}$ and the target distribution $\pi^{(1)}$, we expect to minimize the expected round trip time T (defined in section A.5 (appendix)) to ensure both efficient exploitation and explorations. The non-Markovian nature of the index process makes the analysis challenging. To facilitate the analysis, we treat swap indicators as independent Bernoulli variables following Syed et al. (2021). Combining the Markov property, we estimate the expected round trip time $\mathbb{E}[T]$ as follows:

Lemma 1. *Under the stationary and weak independence assumptions B1 and B2 in section B (appendix), for P ($P \geq 2$) chains with window size W ($W \geq 1$) and rejection rates $\{r_p\}_{p=1}^{P-1}$, we have*

$$\mathbb{E}[T] = 2WP + \underbrace{2WP \sum_{p=1}^{P-1} \frac{r_p^W}{1 - r_p^W}}_{\text{Quadratic term in } P}. \quad (3)$$

The proof in section B.1 shows that $\mathbb{E}[T]$ increases as we adopt larger number of chains P and rejection rates $\{r_p\}_{p=1}^{P-1}$. In such a case, the round trip rate $\frac{P}{\mathbb{E}[T]}$ is also maximized by the key renewal theorem. In particular, applying $W = 1$ recovers the vanilla DEO scheme.

Analysis of optimal window size and round trip time

By Lemma 1, we observe a potential to remove the quadratic term given an appropriate W . Such a fact mo-

tivates us to study the optimal W to achieve the best efficiency. Under the equi-acceptance settings, by treating W as a continuous variable and taking the derivative with respect to W , we have

$$\frac{\partial}{\partial W} \mathbb{E}[T] = \frac{2P}{(1 - r^W)^2} \left\{ (1 - r^W)^2 + (P - 1)r^W(1 - r^W + W \log r) \right\}, \quad (4)$$

where r is the equi-rejection rate for adjacent chains. Define $x := r^W \in (0, 1)$, where $W = \log_r(x) = \frac{\log x}{\log r}$. The following analysis hinges on the study of the solution of $g(x) = (1 - x)^2 + (P - 1)x(1 - x + \log(x)) = 0$. By analyzing the growth of derivatives and boundary values, we can identify the *uniqueness* of the solution. Then, we proceed to verify that $\frac{1}{P \log P}$ yields an asymptotic approximation such that $g(\frac{1}{P \log P}) = -\frac{\log(\log P)}{\log P} + O\left(\frac{1}{\log P}\right) \rightarrow 0$ as $P \rightarrow \infty$. In the end, we have

Theorem 1. *Under Assumptions B1 (Stationarity) and B2 (Weak independence) based on equi-acceptance settings, if $P = 2, 3$, the minimal round trip time is achieved when $W = 1$. If $P \geq 4$, with the optimal window size $W_\star \approx \left\lceil \frac{\log P + \log \log P}{-\log r} \right\rceil$, where $\lceil \cdot \rceil$ is the ceiling function.*

The round trip time follows $O(\frac{P \log P}{-\log r})$.

The above result yields a remarkable round trip time of $O(P \log P)$ by setting the optimal window size W_\star . By contrast, the vanilla DEO scheme only leads to a longer time of $O(P^2)$ §. Denoting by DEO_★ the generalized DEO scheme with the optimal window size W_\star , we summarize the popular swap schemes in Table 1, where the DEO_★ scheme performs the best among all the three criteria. We acknowledge that the assumptions are inevitably strong to simplify the analysis (Syed et al. 2021) due to the intractable index process. Empirically, assumption B1 approximately holds after a sufficient burn-in period; more in-depth discussions on the robustness of assumption B2 have also been evaluated in section 7.2 of Syed et al. (2021).

§By Taylor expansion, given a large rejection rate r , $-\log(r) = 1 - r$, which means $\frac{1}{-\log(r)} = O(\frac{r}{1-r})$.

Table 1: Round trip time and swap time for different schemes. Notably, non-asymptotic refers to cases with large rejection rates due to a limited number of chains; asymptotic occurs given sufficiently many chains such that rejection rates are close to 0. The APE scheme requires an expensive swap time of $O(P^3)$ and is not compared.

	ROUND TRIP TIME (NON-ASYMPTOTIC)	ROUND TRIP TIME (ASYMPTOTIC)	SWAP TIME
ADJ	$O(P^2)$ (NADLER AND HANSMANN 2007B)	$O(P^2)$ (NADLER AND HANSMANN 2007B)	$O(P)$
SEO	$O(P^2)$ (SYED ET AL. 2021)	$O(P^2)$ (SYED ET AL. 2021)	$O(1)$
DEO	$O(P^2)$ (SYED ET AL. 2021)	$O(P)$ (SYED ET AL. 2021)	$O(1)$
DEO _*	$O(P \log P)$	$O(P)$	$O(1)$

Discussions on the optimal number of chains

Note that in practice given P parallel chains, a large P leads to a smaller equi-rejection rate r . As such, we can further obtain a crude estimate of the optimal P to minimize the round trip time.

Corollary 1. *Under Assumptions B1-B4 and C1 under equi-acceptance settings with the optimal window size, the optimal chains follow that $P_* > \min_p \frac{\sigma_p}{3\tau^{(p)}} \log(\frac{\tau^{(P)}}{\tau^{(1)}})$, where σ_p is defined in Eq.(14) (appendix).*

The assumptions and proof are postponed in section B.3 (appendix). In mini-batch settings, insufficient chains may lead to few effective swaps for accelerations; by contrast, introducing too many chains may be too costly in terms of the round trip time. This is different from the conclusion in full-batch settings, where Syed et al. (2021) suggested running the vanilla DEO scheme with as many chains as possible to yield a small enough equi-rejection rate r to maintain the non-reversibility.

Cutoff phenomenon On the one hand, when we only afford at most P chains, where $P < P_*$, a large equi-rejection rate r is inevitable and DEO_{*} is preferred over DEO; on the other hand, the rejection rate r goes to 0 when $P \gg P_*$ and DEO_{*} recovers the DEO scheme.

In section B.4 (appendix), we show that P_* is in the order of thousands for the CIFAR100 example, which is hard to achieve due to the limited computational budget and further motivates us to adopt finite chains with a target swap rate \mathbb{S} to balance between acceleration and accuracy.

User-friendly approximate explorations in big Data

Despite the asymptotic correctness, stochastic gradient Langevin dynamics (Welling and Teh 2011) (SGLD) only works well given *small enough learning rates* and fails in explorative purposes (Ahn, Korattikara, and Welling 2012). A large learning rate, however, leads to excessive stochastic gradient noise and ends up with a crude approximation. As such, similarly to Izmailov et al. (2018); Zhang et al. (2020), we only adopt SGLD for exploitations.

Efficient explorations not only require a high temperature but also prefer a large learning rate. Such a demand

Algorithm 1: Non-reversible parallel tempering with SGD-based exploration kernels (DEO_{*}-SGD).

Input Number of chains $P \geq 3$, boundary learning rates $\eta^{(1)}$ and $\eta^{(P)}$, target swap rate \mathbb{S} .

Input Optimal window size $W := \left\lceil \frac{\log P + \log \log P}{-\log(1-\mathbb{S})} \right\rceil$, total iterations K , and step sizes $\{\gamma_k\}_{k=0}^K$.

for $k = 0$ to K **do**

$\beta_{k+1} \sim \mathcal{T}_\eta(\beta_k)$ following Eq.(6) \triangleright **Sampling phase**

$\mathcal{P} = \{\forall p \in \{1, 2, \dots, P\} : p \bmod 2 = \lfloor \frac{k}{W} \rfloor \bmod 2\}$.

for $p = 1, 2$ to $P - 1$ **do**

$\mathcal{A}^{(p)} := 1_{\tilde{U}(\beta_{k+1}^{(p+1)}) + \mathbb{C}_k < \tilde{U}(\beta_{k+1}^{(p)})}$

if $k \bmod W = 0$ **then**

Open: $\mathcal{G}^{(p)} = 1$. \triangleright **Open the gate to allow swaps**

end if

if $p \in \mathcal{P}$ and $\mathcal{G}^{(p)}$ and $\mathcal{A}^{(p)}$ **then**

Swap: $\beta_{k+1}^{(p)}$ and $\beta_{k+1}^{(p+1)}$. \triangleright **Communication phase**

Freeze: $\mathcal{G}^{(p)} = 0$. \triangleright **Close the gate to refuse swaps**

end if

if $p > 1$ **then**

Update learning rate (temperature) following Eq.(11)

end if

end for

Correction: $\mathbb{C}_{k+1} = \mathbb{C}_k + \gamma_k \left(\frac{1}{P-1} \sum_{p=1}^{P-1} \mathcal{A}^{(p)} - \mathbb{S} \right)$.

end for

Output Target models $\{\beta_k^{(1)}\}_{k=1}^K$.

inspires us to consider SGD with a constant learning rate η as the exploration component

$$\begin{aligned} \beta_{k+1} &= \beta_k - \eta \nabla \tilde{U}(\beta_k) = \beta_k - \eta (\nabla U(\beta_k) + \varepsilon(\beta_k)) \\ &= \beta_k - \eta \nabla U(\beta_k) - \sqrt{2\eta \left(\frac{\eta}{2}\right)} \varepsilon(\beta_k), \end{aligned} \tag{5}$$

where $\tilde{U}(\cdot)$ is the unbiased energy estimate of $U(\cdot)$ and $\varepsilon(\beta_k) \in \mathbb{R}^d$ is the stochastic gradient noise with mean 0. Under mild normality assumptions on ε (Mandt, Hoffman, and Blei 2017; Chen et al. 2020), β_k converges approximately to an invariant distribution, where the underlying temperature linearly depends on the learning rate η . Motivated by this fact, we propose an approximate transition kernel \mathcal{T}_η with P parallel SGD runs

based on different learning rates

$$\begin{aligned} \text{Exploration: } & \begin{cases} \beta_{k+1}^{(P)} = \beta_k^{(P)} - \eta^{(P)} \nabla \tilde{U}(\beta_k^{(P)}), \\ \dots \\ \beta_{k+1}^{(2)} = \beta_k^{(2)} - \eta^{(2)} \nabla \tilde{U}(\beta_k^{(2)}), \end{cases} \\ \text{Exploitation: } & \beta_{k+1}^{(1)} = \beta_k^{(1)} - \eta^{(1)} \nabla \tilde{U}(\beta_k^{(1)}) + \overbrace{\Xi_k}^{\text{optional}}, \end{aligned} \quad (6)$$

where $\eta^{(1)} < \eta^{(2)} < \dots < \eta^{(P)}$, $\Xi_k \sim \mathcal{N}(0, 2\eta^{(1)}\tau^{(1)})$, and $\tau^{(1)}$ is the target temperature.

Since there exists an optimal learning rate for SGD to estimate the desired distribution through Laplace approximation (Mandt, Hoffman, and Blei 2017), the exploitation kernel can be also replaced with SGD based on constant learning rates if the accuracy demand is not high. Regarding the validity of adopting different learning rates for parallel tempering, we leave discussions to section A.2 (appendix).

Approximation analysis

Moreover, the stochastic gradient noise exploits the Fisher information (Ahn, Korattikara, and Welling 2012; Zhu et al. 2019; Chaudhari et al. 2017) and yields convergence potential to wide optima with good generalizations (Berthier, Bach, and Gaillard 2020; Zou et al. 2021). Despite the implementation convenience, the inclusion of SGDs has made the temperature variable inaccessible, rendering a difficulty in implementing the Metropolis rule Eq.(2). To tackle this issue, we utilize the randomness in stochastic energies and propose a *deterministic swap condition* for the approximate kernel \mathcal{T}_η in Eq.(6)

$$\begin{aligned} \text{Deterministic swap condition: } & \text{if } \tilde{U}(\beta^{(p+1)}) + \mathbb{C} < \tilde{U}(\beta^{(p)}) \\ & (\beta^{(p)}, \beta^{(p+1)}) \rightarrow (\beta^{(p+1)}, \beta^{(p)}), \end{aligned} \quad (7)$$

where $p \in \{1, 2, \dots, P-1\}$, $\mathbb{C} > 0$ is a correction buffer to approximate the Metropolis rule Eq.(2).

Lemma 2. *Assume the energy normality assumption (C1), then for any fixed $\partial U_p := U(\beta^{(p)}) - U(\beta^{(p+1)})$, there exists an optimal $\mathbb{C}_* \in (0, (\frac{1}{\tau^{(p)}} - \frac{1}{\tau^{(p+1)}})\sigma_p^2]$ that perfectly approximates the random event $\tilde{S}(\beta^{(p)}, \beta^{(p+1)}) > u$, where σ_p defined in Eq.(14) (appendix) and $u \sim \text{Unif}[0, 1]$.*

The proof is postponed in section C.1 (appendix), which paves the way for the guarantee that a *deterministic swap condition* may replace the Metropolis rule Eq.(2) for approximations. In addition, the normality assumption can be naturally extended to the asymptotic normality assumption (Quiroz et al. 2019; Deng et al. 2021) given large enough batch sizes.

Admittedly, the approximation error still exists for different ∂U_p . By the mean-value theorem, there exists a tunable \mathbb{C} to optimize the overall approximation. Further invoking the central limit theorem such that $\varepsilon(\cdot)$ in Eq.(5)

approximates a Gaussian distribution with a fixed covariance, we can expect a bounded approximation error for the SGD-based exploration kernels (Mandt, Hoffman, and Blei 2017).

Theorem 2. *Consider the exact transition kernel \mathcal{T} and the proposed approximate kernel \mathcal{T}_η , which yield stationary distributions π and π_η , respectively. Under smoothness (C2) and dissipativity assumptions (C3) (Mattingly, Stuart, and Higham 2002; Raginsky, Rakhlin, and Telgarsky 2017; Xu et al. 2018), \mathcal{T} satisfies the geometric ergodicity such that there is a contraction constant $\rho \in [0, 1)$ for any distribution μ :*

$$\|\mu\mathcal{T} - \pi\|_{TV} \leq \rho\|\mu - \pi\|_{TV},$$

where $\|\cdot\|_{TV}$ is the total variation (TV) distance. Moreover, assume that $\varepsilon(\cdot) \sim \mathcal{N}(0, \mathcal{M})$ for some positive definite matrix \mathcal{M} (C4) (Mandt, Hoffman, and Blei 2017), then there is a uniform upper bound of the one step error between \mathcal{T} and \mathcal{T}_η such that

$$\|\mu\mathcal{T} - \mu\mathcal{T}_\eta\|_{TV} \leq \Delta_{\max}, \forall \mu,$$

where $\Delta_{\max} \geq 0$ is a constant. Eventually, the TV distance between π and π_η is bounded by

$$\|\pi - \pi_\eta\|_{TV} \leq \frac{\Delta_{\max}}{1 - \rho}.$$

The proof is postponed to section C.2 (appendix). The SGD-based exploration kernels *no longer require to fine-tune the temperatures* directly and naturally inherits the empirical successes of SGD in large-scale deep learning tasks. The inaccessible Metropolis rule Eq.(2) is approximated via the *deterministic swap condition* Eq.(7) and leads to robust approximations by tuning $\eta = (\eta^{(1)}, \dots, \eta^{(P)})$ and \mathbb{C} .

In addition, our proposed algorithm for posterior approximation also relates to non-convex optimization. For detailed discussions, we refer interested readers to section A.4 (appendix).

Equi-acceptance parallel tempering on optimized paths

Stochastic approximation (SA) is a standard method to achieve equi-acceptance (Atchadé, Roberts, and Rosenthal 2011; Miasojedow, Éric Moulines, and Vihola 2013), however, implementing this idea with fixed $\eta^{(1)}$ and $\eta^{(P)}$ is rather non-trivial. Motivated by the linear relation between learning rate and temperature, we propose to adaptively *optimize the learning rates* to achieve equi-acceptance in a user-friendly manner. Further by the geometric temperature spacing commonly adopted by practitioners (Kofke 2002; Earl and Deem 2005; Syed et al. 2021), we adopt the following scheme on a *logarithmic scale*

$$\partial \log(v_t^{(p)}) = h^{(p)}(v_t^{(p)}), \quad (8)$$

where $p \in \{1, 2, \dots, P-1\}$, $v_t^{(p)} = \eta_t^{(p+1)} - \eta_t^{(p)}$, $h^{(p)}(v_t^{(p)}) := \int H^{(p)}(v_k^{(p)}, \beta) \pi^{(p,p+1)}(d\beta)$ is the

mean-field function, $\pi^{(p,p+1)}$ is the joint invariant distribution for the p -th and $p+1$ -th processes. In particular, $H^{(p)}(v_k^{(p)}, \beta) = 1_{\tilde{U}(\beta^{(p+1)}) + \mathbb{C} < \tilde{U}(\beta^{(p)})} - \mathbb{S}$ is the random-field function to approximate $h^{(p)}(v_k^{(p)})$ with limited perturbations, $v_k^{(p) \dagger}$ implicitly affects the distribution of the indicator function, and \mathbb{S} is the target swap rate. Now consider stochastic approximation of Eq.(8), we have

$$\log(v_{k+1}^{(p)}) = \log(v_k^{(p)}) + \gamma_k H^{(p)}(v_k^{(p)}, \beta_k), \quad (9)$$

where γ_k is the step size. Reformulating Eq.(9), we have

$$v_{k+1}^{(p)} = \max(0, v_k^{(p)}) e^{\gamma_k H^{(p)}(v_k^{(p)})},$$

where the max operator is conducted explicitly to ensure the sequence of learning rates is non-decreasing. This means given fixed boundary learning rates (temperatures) $\eta_k^{(p-1)}$ and $\eta_k^{(p+1)}$, applying $\eta^{(p)} = \eta^{(p-1)} + v^{(p)}$ and $\eta^{(p)} = \eta^{(p+1)} - v^{(p+1)}$ for $p \in \{2, 3, \dots, P-1\}$ lead to

$$\begin{aligned} \eta_{k+1}^{(p)} &= \underbrace{\eta_k^{(p-1)} + \max(0, v_k^{(p)}) e^{\gamma_k H^{(p)}(v_k^{(p)})}}_{\text{forward sequence}} \\ &= \underbrace{\eta_k^{(p+1)} - \max(0, v_k^{(p+1)}) e^{\gamma_k H^{(p)}(v_k^{(p+1)})}}_{\text{backward sequence}}. \end{aligned} \quad (10)$$

Adaptive learning rates (temperatures) Now given a fixed $\eta^{(1)}$, the sequence $\eta^{(2)}, \eta^{(3)}, \dots, \eta^{(P)}$ can be approximated iteratively via the forward sequence of (10); conversely, given a fixed $\eta^{(P)}$, the backward sequence $\eta^{(P-1)}, \eta^{(P-2)}, \dots, \eta^{(1)}$ can be decided reversely as well. Combining the forward and backward sequences, $\eta_{k+1}^{(p)}$ can be approximated via

$$\begin{aligned} \eta_{k+1}^{(p)} &:= \frac{\eta_k^{(p-1)} + \eta_k^{(p+1)}}{2} + \\ &\frac{\max(0, v_k^{(p)}) e^{\gamma_k H^{(p)}(v_k^{(p)})} - \max(0, v_k^{(p+1)}) e^{\gamma_k H^{(p)}(v_k^{(p+1)})}}{2}, \end{aligned} \quad (11)$$

which resembles the *binary search* in the SA framework. In particular, the first term is the middle point given boundary learning rates and the second term continues to penalize learning rates that violates the equi-acceptance between pairs $(p-1, p)$ and $(p, p+1)$ until an equilibrium is achieved.

This is the first attempt to achieve equi-acceptance given two fixed boundary values to our best knowledge. By contrast, Syed et al. (2021) proposed to estimate the barrier Λ to determine the temperatures and it easily fails in big data given a finite number of chains and bias-corrected swaps.

$\dagger v_t^{(p)}$ denotes a continuous-time diffusion at time t and $v_k^{(p)}$ is a discrete approximation at iteration k .

Adaptive correction buffers In addition, equi-acceptance does not guarantee a convergence to the desired acceptance rate \mathbb{S} . To avoid this issue, we propose to adaptively optimize \mathbb{C} as follows

$$\mathbb{C}_{k+1} = \mathbb{C}_k + \gamma_k \left(\frac{1}{P-1} \sum_{p=1}^{P-1} 1_{\tilde{U}(\beta_{k+1}^{(p+1)}) + \mathbb{C}_k - \tilde{U}(\beta_{k+1}^{(p)}) < 0} - \mathbb{S} \right). \quad (12)$$

As $k \rightarrow \infty$, the threshold and the adaptive learning rates converge to the desired fixed points. Note that setting a uniform \mathbb{C} greatly simplifies the algorithm. Now we refer to the approximate non-reversible parallel tempering algorithm with the DEO_{*} scheme and SGD-based exploration kernels as DEO_{*}-SGD and formally formulate our algorithm in Algorithm 1. Extensions of SGD with a preconditioner (Li et al. 2016) or momentum (Chen, Fox, and Guestrin 2014) to further improve the approximation and efficiency are both straightforward (Mandt, Hoffman, and Blei 2017) and are denoted as DEO_{*}-pSGD and DEO_{*}-mSGD, respectively.

Experiments

Simulations of multi-modal distributions

We first simulate the proposed algorithm on a distribution $\pi(\beta) \propto \exp(-U(\beta))$, where $\beta = (\beta_1, \beta_2)$, $U(\beta) = 0.2(\beta_1^2 + \beta_2^2) - 2(\cos(2\pi\beta_1) + \cos(2\pi\beta_2))$. The heat map is shown in Figure 3(a) with 25 modes of different volumes. To mimic big data scenarios, we can only access stochastic gradient $\nabla \tilde{U}(\beta) = \nabla U(\beta) + 2\mathcal{N}(0, \mathbf{I}_{2 \times 2})$ and stochastic energy $\tilde{U}(\beta) = U(\beta) + 2\mathcal{N}(0, I)$.

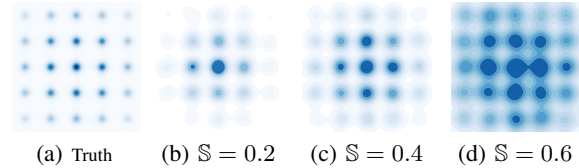


Figure 3: Study of different target swap rate \mathbb{S} via DEO_{*}-SGD, where SGLD is the exploitation kernel.

We first run DEO_{*}-SGD \times P16 based on 16 chains and 20,000 iterations. We fix the lowest learning rate 0.003 and the highest learning 0.6 and propose to tune the target swap rate \mathbb{S} for the acceleration-accuracy trade-off. Figure 3 shows that fixing $\mathbb{S} = 0.2$ is too conservative and underestimates the uncertainty on the corners; $\mathbb{S} = 0.6$ results in too many radical swaps and eventually leads to crude estimations; by contrast, $\mathbb{S} = 0.4$ yields the best posterior approximation among the five choices.

Next, we select $\mathbb{S} = 0.4$ and study the round trips. We observe in Figure 4(a) that the vanilla DEO only yields 18 round trips every 1,000 iterations; by contrast, slightly increasing W tends to improve the efficiency significantly and the optimal 45 round trips are achieved at $W = 8$, which *matches our theory*. In Figure 4(b-c), the geometrically initialized learning rates lead to unbalanced acceptance rates in the early phase and some

Table 2: posterior approximation and optimization on CIFAR100 via $10\times$ budget.

MODEL	ResNet20		ResNet32		ResNet56	
	NLL	ACC (%)	NLL	ACC (%)	NLL	ACC (%)
cycSGHMC \times T10	8198 \pm 59	76.26 \pm 0.18	7401 \pm 28	78.54 \pm 0.15	6460 \pm 21	81.78 \pm 0.08
cycSWAG \times T10	8164 \pm 38	76.13 \pm 0.21	7389 \pm 32	78.62 \pm 0.13	6486 \pm 29	81.60 \pm 0.14
mSGD \times P10	7902 \pm 64	76.59 \pm 0.11	7204 \pm 29	79.02 \pm 0.09	6553 \pm 15	81.49 \pm 0.09
DEO-mSGD \times P10	7964 \pm 23	76.84 \pm 0.12	7152 \pm 41	79.34 \pm 0.15	6534 \pm 26	81.72 \pm 0.12
DEO $_{\star}$ -mSGD \times P10	7741\pm67	77.37\pm0.16	7019\pm35	79.54\pm0.12	6439\pm32	82.02\pm0.15

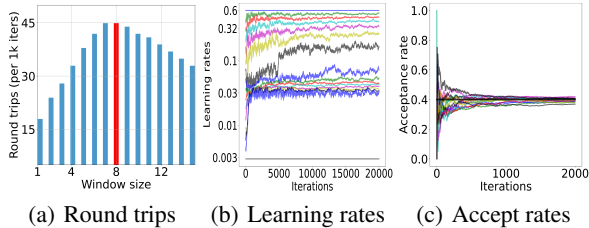


Figure 4: Study of window sizes, learning rates, acceptance rates, and the corrections.

adjacent chains have few swaps and others swap too much, but as the optimization proceeds, the learning rates gradually converge.

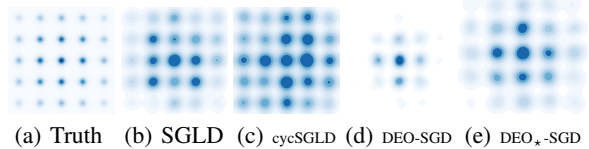


Figure 5: Simulations of the multi-modal distribution through different sampling algorithms. All the algorithms are run based on 16 chains \times P16

We compare the proposed algorithm with parallel SGLD based on 20,000 iterations and 16 chains (SGLD \times P16); we fix the learning rate 0.003 and a temperature 1. We also run cycSGLD \times T16, which denotes a single chain based on 16 times of budget and cosine learning rates (Zhang et al. 2020) of 100 cycles. We see in Figure 5(b) that SGLD \times P16 has good explorations but fails to approximate the posterior. Figure 5(c) shows that cycSGLD \times T16 explores most of the modes but overestimates some areas occasionally. Figure 5(d) demonstrates the DEO-SGD with 16 chains (DEO-SGD \times P16) estimates the uncertainty of the centering 9 modes well but fails to deal with the rest of the modes. As to DEO $_{\star}$ -SGD \times P16, the approximation is rather accurate, as shown in Figure 5(e).

We also present the index process for both schemes in Figure 6. The vanilla DEO scheme results in volatile paths and a particle takes quite a long time to complete a round trip; by contrast, DEO $_{\star}$ only conducts at most one cheap swap in a window and yields much more

deterministic paths.

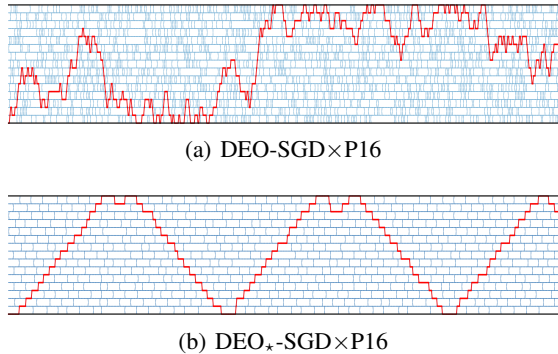


Figure 6: Dynamics of the index process. The red path denotes the round trip path for a particle.

Posterior approximation for image data

Next, we conduct experiments on computer vision tasks. We choose ResNet20, ResNet32, and ResNet56 (He et al. 2016) and train the models on CIFAR100. We report negative log likelihood (NLL) and test accuracy (ACC). For each model, we first pre-train 10 fixed models via 300 epochs and then run algorithms based on momentum SGD (mSGD) for 500 epochs with 10 parallel chains and denote it by DEO $_{\star}$ -mSGD \times P10. We fix the lowest and highest learning rates as 0.005 and 0.02, respectively. For a fair comparison, we also include the baseline DEO-mSGD \times P10 with the same setup except that the window size is 1; the standard ensemble mSGD \times P10 is also included with a learning rate of 0.005. In addition, we include two baselines based on a single long chain, i.e. we run stochastic gradient Hamiltonian Monte Carlo (Chen, Fox, and Guestrin 2014) 5000 epochs with cyclical learning rates and 50 cycles (Zhang et al. 2020) and refer to it as cycSGHMC \times T10; we run SWAG \times T10 (Maddox et al. 2019) under similar setups.

In particular for DEO $_{\star}$ -mSGD \times P10, we tune the target swap rate \mathbb{S} and find an optimum at $\mathbb{S} = 0.005$. We compare our proposed algorithm with the four baselines and observe in Table 2 that mSGD \times P10 can easily obtain competitive results simply through model ensemble (Lakshminarayanan, Pritzel, and Blundell 2017), which outperforms cycSGHMC \times T10 and cycSWAG \times T10 on ResNet20 and ResNet32 models and

perform the worst among the five methods on ResNet56; DEO-mSGD×P10 itself is already a pretty powerful algorithm, however, DEO_{*}-mSGD×P10 consistently outperforms the vanilla alternative.

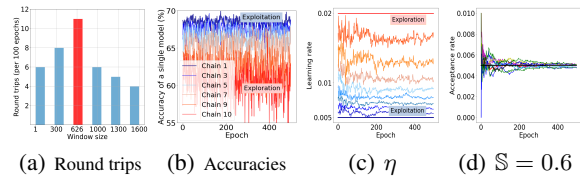


Figure 7: Study of window sizes, accuracies, learning rates (η), and acceptance rates (\mathbb{S}) on ResNet20.

To analyze why the proposed scheme performs well, we study the round trips in Figure 7(a) and find that the theoretical optimal window obtains around 11 round trips every 100 epochs, which is almost 2 times as much as DEO. In Figure 7(b), we observe that the smallest learning rate obtains the highest accuracy (blue) for exploitations, while the largest learning rate yields decent explorations (red); we see in Figure 7(c) and 7(d) that geometrically initialized learning rates converge to fixed points and the acceptance rates converge to the target.

Conclusion

In this paper, we show how to adapt the multiple-chain parallel tempering algorithm to big data problems. Given a limited budget of parallel chains in big data, we show the standard non-reversible DEO scheme leads to an expensive quadratic communication cost with respect to the number of chains. To tackle that issue, we propose a generalized DEO scheme to achieve larger swap rates (window-wise) with mild costs. By sacrificing a mild accuracy in big data, we prove the existence of an optimal window size to encourage *deterministic paths* and obtain in a significant *acceleration of $O(\frac{P}{\log P})$ times*. For a user-friendly purpose, we also propose a deterministic swap condition to interact with SGD-based exploration kernels. A crude bias analysis is provided to facilitate the understanding of the extensions.

Acknowledgments

Lin and Deng would like to acknowledge the support from National Science Foundation (DMS-2053746, DMS-1555072, and DMS-1736364), Brookhaven National Laboratory Subcontract (382247), and U.S. Department of Energy Office of Science Advanced Scientific Computing Research (DE-SC0021142). Liang’s research is supported in part by the grant DMS-2015498 from National Science Foundation and the grants R01-GM117597 and R01-GM126089 from National Institutes of Health.

References

Ahn, S.; Korattikara, A.; and Welling, M. 2012. Bayesian Posterior Sampling via Stochastic Gradient Fisher Scor-

ing. In *Proc. of the International Conference on Machine Learning (ICML)*.

Aitchison, L. 2021. A Statistical Theory of Cold Posteriors in Deep Neural Networks. In *Proc. of the International Conference on Learning Representation (ICLR)*.

Atchadé, Y. F.; Roberts, G. O.; and Rosenthal, J. S. 2011. Towards Optimal Scaling of Metropolis-coupled Markov Chain Monte Carlo. *Statistics and Computing*, 21: 555–568.

Bardenet, R.; Doucet, A.; and Holmes, C. 2017. On Markov Chain Monte Carlo Methods for Tall Data. *Journal of Machine Learning Research*, 18: 1–43.

Berthier, R.; Bach, F.; and Gaillard, P. 2020. Tight Non-parametric Convergence Rates for Stochastic Gradient Descent under the Noiseless Linear Model. In *Advances in Neural Information Processing Systems (NeurIPS)*.

Brenner, P.; Sweet, C. R.; VonHandorf, D.; and Izaguirre, J. A. 2007. Accelerating the Replica Exchange Method through an Efficient All-pairs Exchange. *The Journal of Chemical Physics*, 126: 074103.

Ceperley, D.; and Dewing, M. 1999. The Penalty Method for Random Walks with Uncertain Energies. *The Journal of Chemical Physics*, 110: 9812–9820.

Chaudhari, P.; Choromanska, A.; Soatto, S.; LeCun, Y.; Baldassi, C.; Borgs, C.; Chayes, J.; Sagun, L.; and Zecchina, R. 2017. Entropy-SGD: Biasing Gradient Descent Into Wide Valleys. In *Proc. of the International Conference on Learning Representation (ICLR)*.

Chen, T.; Fox, E. B.; and Guestrin, C. 2014. Stochastic Gradient Hamiltonian Monte Carlo. In *Proc. of the International Conference on Machine Learning (ICML)*.

Chen, X.; Lee, J. D.; Tong, X. T.; and Zhang, Y. 2020. Statistical Inference for Model Parameters in Stochastic Gradient Descent. *Annals of Statistics*, 48(1): 251–273.

Chen, Y.; Chen, J.; Dong, J.; Peng, J.; and Wang, Z. 2019. Accelerating Nonconvex Learning via Replica Exchange Langevin Diffusion. In *Proc. of the International Conference on Learning Representation (ICLR)*.

Csiszár, I.; and Körner, J. 2011. *Information Theory: Coding Theorems for Discrete Memoryless Systems*. Cambridge University Press.

Dalalyan, A. S. 2017. Theoretical Guarantees for Approximate Sampling from Smooth and Log-concave Densities. *Journal of the Royal Statistical Society: Series B*, 79(3): 651–676.

Deng, W.; Feng, Q.; Gao, L.; Liang, F.; and Lin, G. 2020. Non-Convex Learning via Replica Exchange Stochastic Gradient MCMC. In *Proc. of the International Conference on Machine Learning (ICML)*.

Deng, W.; Feng, Q.; Karagiannis, G.; Lin, G.; and Liang, F. 2021. Accelerating Convergence of Replica Exchange Stochastic Gradient MCMC via Variance Reduction. In *Proc. of the International Conference on Learning Representation (ICLR)*.

Deng, W.; Liang, S.; Hao, B.; Lin, G.; and Liang, F. 2022. Interacting Contour Stochastic Gradient Langevin

- Dynamics. In *Proc. of the International Conference on Learning Representation (ICLR)*.
- Deng, W.; Lin, G.; and Liang, F. 2022. An Adaptively Weighted Stochastic Gradient MCMC Algorithm for Monte Carlo Simulation and Global Optimization. *Statistics and Computing*, 32–58.
- Dong, J.; and Tong, X. T. 2021. Replica Exchange for Non-Convex Optimization. *arXiv:2001.08356v4*.
- Dupuis, P.; Liu, Y.; Plattner, N.; and Doll, J. D. 2012. On the Infinite Swapping Limit for Parallel Tempering. *SIAM J. Multiscale Modeling & Simulation*, 10.
- Durmus, A.; and Moulines, E. 2016. Sampling from a Strongly Log-concave Distribution with the Unadjusted Langevin Algorithm. *arXiv:1605.01559*.
- Earl, D. J.; and Deem, M. W. 2005. Parallel Tempering: Theory, Applications, and New Perspectives. *Phys. Chem. Chem. Phys.*, 7: 3910–3916.
- Gelman, A.; Gilks, W. R.; and Roberts, G. O. 1997. Weak Convergence and Optimal Scaling of Random Walk Metropolis Algorithms. *Annals of Applied Probability*, 7: 110–120.
- Gerber, H. U.; Shiu, E. S. W.; and Yang, H. 2015. Geometric Stopping of a Random Walk and Its Applications to Valuing Equity-linked Death Benefits. *Insurance: Mathematics and Economics*, 64: 313–325.
- He, K.; Zhang, X.; Ren, S.; and Sun, J. 2016. Deep Residual Learning for Image Recognition. In *The IEEE Conference on Computer Vision and Pattern Recognition (CVPR)*.
- Izmailov, P.; Podoprikin, D.; Garipov, T.; Vetrov, D.; and Wilson, A. G. 2018. Averaging Weights Leads to Wider Optima and Better Generalization. In *Proc. of the Conference on Uncertainty in Artificial Intelligence (UAI)*.
- Kofke, D. A. 2002. On the Acceptance Probability of Replica-Exchange Monte Carlo Trials. *The Journal of Chemical Physics*, 117.
- Kone, A.; and Kofke, D. A. 2005. Selection of Temperature Intervals for Parallel-tempering Simulations. *The Journal of Chemical Physics*, 122: 206101.
- Korattikara, A.; Chen, Y.; and Welling, M. 2014. Austerity in MCMC Land: Cutting the Metropolis-Hastings Budget. In *Proc. of the International Conference on Machine Learning (ICML)*.
- Lakshminarayanan, B.; Pritzel, A.; and Blundell, C. 2017. Simple and Scalable Predictive Uncertainty Estimation using Deep Ensemble. In *Advances in Neural Information Processing Systems (NeurIPS)*.
- Li, C.; Chen, C.; Carlson, D.; and Carin, L. 2016. Pre-conditioned Stochastic Gradient Langevin Dynamics for Deep Neural Networks. In *Proc. of the National Conference on Artificial Intelligence (AAAI)*, 1788–1794.
- Lingenheil, M.; Denschlag, R.; Mathias, G.; and Tavan, P. 2009. Efficiency of Exchange Schemes in Replica Exchange. *Chemical Physics Letters*, 478: 80–84.
- Liu, Q.; and Wang, D. 2016. Stein Variational Gradient Descent: A General Purpose Bayesian Inference Algorithm. In *Advances in Neural Information Processing Systems (NeurIPS)*.
- Maddox, W.; Garipov, T.; Izmailov, P.; Vetrov, D.; and Wilson, A. G. 2019. A Simple Baseline for Bayesian Uncertainty in Deep Learning. In *Advances in Neural Information Processing Systems (NeurIPS)*.
- Mandt, S.; Hoffman, M. D.; and Blei, D. M. 2017. Stochastic Gradient Descent as Approximate Bayesian Inference. *Journal of Machine Learning Research*, 18: 1–35.
- Mangoubi, O.; and Vishnoi, N. K. 2018. Convex Optimization with Unbounded Nonconvex Oracles using Simulated Annealing. In *Proc. of Conference on Learning Theory (COLT)*.
- Mattngly, J.; Stuart, A.; and Higham, D. 2002. Ergodicity for SDEs and Approximations: Locally Lipschitz Vector Fields and Degenerate Noise. *Stochastic Processes and their Applications*, 101: 185–232.
- Miasojedow, B.; Éric Moulines; and Vihola, M. 2013. An Adaptive Parallel Tempering Algorithm. *Journal of Computational and Graphical Statistics*, 22(3): 649–664.
- Nadler, W.; and Hansmann, U. H. E. 2007a. Dynamics and Optimal Number of Replicas in Parallel Tempering Simulations. *Phys. Rev. E*, 76: 065701.
- Nadler, W.; and Hansmann, U. H. E. 2007b. Generalized Ensemble and Tempering Simulations: A Unified View. *Phys. Rev. E*, 75: 026109.
- Okabe, T.; Kawata, M.; Okamoto, Y.; and Mikami, M. 2001. Replica Exchange Monte Carlo Method for the Isobaric–isothermal Ensemble. *Chemical Physics Letters*, 335: 435–439.
- Predescu, C.; Predescu, M.; and Ciobanu, C. V. 2004. The Incomplete Beta Function Law for Parallel Tempering Sampling of Classical Canonical Systems. *Chemical Physics Letters*, 120: 4119–4128.
- Quiroz, M.; Kohn, R.; Villani, M.; and Tran, M.-N. 2019. Speeding Up MCMC by Efficient Data Subsampling. *Journal of the American Statistical Association*, 114: 831–843.
- Raginsky, M.; Rakhlin, A.; and Telgarsky, M. 2017. Non-convex Learning via Stochastic Gradient Langevin Dynamics: a Nonasymptotic Analysis. In *Proc. of Conference on Learning Theory (COLT)*.
- Robbins, H.; and Monroe, S. 1951. A Stochastic Approximation Method. *The Annals of Mathematical Statistics*, 22(3): 400–407.
- Sato, I.; and Nakagawa, H. 2014. Approximation Analysis of Stochastic Gradient Langevin Dynamics by Using Fokker-Planck Equation and Ito Process. In *Proc. of the International Conference on Machine Learning (ICML)*.
- Seita, D.; Pan, X.; Chen, H.; and Canny, J. 2017. An Efficient Minibatch Acceptance Test for Metropolis-Hastings. In *Proc. of the Conference on Uncertainty in Artificial Intelligence (UAI)*.

Syed, S.; Bouchard-Côté, A.; Deligiannidis, G.; and Doucet, A. 2021. Non-Reversible Parallel Tempering: a Scalable Highly Parallel MCMC scheme. *Journal of the Royal Statistical Society: Series B*, 84: 321–350.

Welling, M.; and Teh, Y. W. 2011. Bayesian Learning via Stochastic Gradient Langevin Dynamics. In *Proc. of the International Conference on Machine Learning (ICML)*, 681–688.

Wenzel, F.; Roth, K.; Veeling, B. S.; Światkowski, J.; Tran, L.; Mandt, S.; Snoek, J.; Salimans, T.; Jenatton, R.; and Nowozin, S. 2020. How Good is the Bayes Posterior in Deep Neural Networks Really? In *Proc. of the International Conference on Machine Learning (ICML)*.

Xu, P.; Chen, J.; Zou, D.; and Gu, Q. 2018. Global Convergence of Langevin Dynamics Based Algorithms for Nonconvex Optimization. In *Advances in Neural Information Processing Systems (NeurIPS)*.

Zhang, R.; Li, C.; Zhang, J.; Chen, C.; and Wilson, A. G. 2020. Cyclical Stochastic Gradient MCMC for Bayesian Deep Learning. In *Proc. of the International Conference on Learning Representation (ICLR)*.

Zhu, Z.; Wu, J.; Yu, B.; Wu, L.; and Ma, J. 2019. The Anisotropic Noise in Stochastic Gradient Descent: Its Behavior of Escaping from Sharp Minima and Regularization Effects. In *Proc. of the International Conference on Machine Learning (ICML)*.

Zou, D.; Wu, J.; Braverman, V.; Gu, Q.; and Kakade, S. M. 2021. Benign Overfitting of Constant-Stepsize SGD for Linear Regression. In *Proc. of Conference on Learning Theory (COLT)*.

Background

Replica exchange stochastic gradient Langevin dynamics

To approximate the replica exchange Langevin diffusion Eq.(1) based on multiple particles $(\beta_{k+1}^{(1)}, \beta_{k+1}^{(2)}, \dots, \beta_{k+1}^{(P)})$ in big data scenarios, replica exchange stochastic gradient Langevin dynamics (reSGLD) proposes the following numerical scheme:

$$\begin{aligned} \text{Exploration: } & \begin{cases} \beta_{k+1}^{(P)} = \beta_k^{(P)} - \eta^{(P)} \nabla \tilde{U}(\beta_k^{(P)}) + \sqrt{2\eta^{(P)}\tau^{(P)}} \xi_k^{(P)}, \\ \dots \\ \beta_{k+1}^{(2)} = \beta_k^{(2)} - \eta^{(2)} \nabla \tilde{U}(\beta_k^{(2)}) + \sqrt{2\eta^{(2)}\tau^{(2)}} \xi_k^{(2)}, \end{cases} \\ \text{Exploitation: } & \beta_{k+1}^{(1)} = \beta_k^{(1)} - \eta^{(1)} \nabla \tilde{U}(\beta_k^{(1)}) + \sqrt{2\eta^{(1)}\tau^{(1)}} \xi_k^{(1)}, \end{aligned} \quad (13)$$

where $\eta^{(\cdot)}$ is the learning rate, $\xi_k^{(\cdot)}$ is a standard d -dimensional Gaussian noise and each subprocess follows a stochastic gradient Langevin dynamics (SGLD) (Welling and Teh 2011). Further assuming the energy normality assumption C1 in section , there exists a σ_p such that

$$\tilde{U}(\beta^{(p)}) - \tilde{U}(\beta^{(p+1)}) \sim \mathcal{N}(U(\beta^{(p)}) - U(\beta^{(p+1)}), 2\sigma_p^2), \text{ for any } \beta^{(p)} \sim \pi^{(p)}, \quad (14)$$

where $p \in \{1, 2, \dots, P-1\}$, in what follows, (Deng et al. 2020) proposed the bias-corrected swap function as follows

$$a\tilde{S}(\beta_{k+1}^{(p)}, \beta_{k+1}^{(p+1)}) = a \cdot \left(1 \wedge e^{\left(\frac{1}{\tau^{(p)}} - \frac{1}{\tau^{(p+1)}}\right) \left(\tilde{U}(\beta_{k+1}^{(p)}) - \tilde{U}(\beta_{k+1}^{(p+1)}) - \left(\frac{1}{\tau^{(p)}} - \frac{1}{\tau^{(p+1)}}\right) \sigma_p^2\right)} \right), \quad (15)$$

where $p \in \{1, 2, \dots, P-1\}$, $\left(\frac{1}{\tau^{(p)}} - \frac{1}{\tau^{(p+1)}}\right) \sigma_p^2$ is a correction term to avoid the bias and the swap intensity a can be then set to $\frac{1}{\min\{\eta^{(p)}, \eta^{(p+1)}\}}$ for convenience. Namely, given a particle pair at location $(\beta^{(p)}, \beta^{(p+1)})$ in the k -th iteration, the conditional probability of the swap follows that

$$\begin{aligned} \mathbb{P}(\beta_{k+1} = (\beta^{(p+1)}, \beta^{(p)}) | \beta_k = (\beta^{(p)}, \beta^{(p+1)})) &= \tilde{S}(\beta^{(p)}, \beta^{(p+1)}), \\ \mathbb{P}(\beta_{k+1} = (\beta^{(p)}, \beta^{(p+1)}) | \beta_k = (\beta^{(p)}, \beta^{(p+1)})) &= 1 - \tilde{S}(\beta^{(p)}, \beta^{(p+1)}). \end{aligned}$$

Inhomogenous swap intensity via different learning rates

Assume the high-temperature process also applies $\eta^{(p+1)} \geq \eta^{(p)} > 0$, where $p \in \{1, 2, \dots, P-1\}$. At time t , the swap intensity can be interpreted as being 0 in a time interval $[t, t + \eta^{(p+1)} - \eta^{(p)})$ and being $\frac{1}{\eta^{(p)}}$ in $[t + \eta^{(p+1)} - \eta^{(p)}, t + \eta^{(p+1)})$. Since the coupled Langevin diffusion process converges to the same joint distribution regardless of the swaps and the swap intensity a varies in a bounded domain, the convergence of numerical schemes is not much affected except the numerical error.

Accuracy-acceleration trade-off

Despite the exponential acceleration potential, the average bias-corrected swap rate is significantly reduced such that $\mathbb{E}[\tilde{S}] = O\left(S e^{-\left(\frac{1}{\tau^{(p)}} - \frac{1}{\tau^{(p+1)}}\right)^2 \frac{\sigma_p^2}{8}}\right)$ (Deng et al. 2021), where S is the swap function following Eq.(2) in full-batch settings. Including more parallel chains is promising to alleviate this issue, however, it is often inevitable to sacrifice some accuracy to obtain more swaps and accelerations, as discussed in section . As such, it inspires us to devise the user-friendly SGD-based approximate exploration kernels.

Connection to non-convex optimization

Parallel to our work, a similar SGLD \times SGD framework was proposed by Dong and Tong (2021) for non-convex optimization, where SGLD and SGD work as exploration and exploitation kernels, respectively. By contrast, our algorithm performs *exactly in the opposite* for posterior approximation because SGLD is theoretically more appealing for the exploitations based on small learning rates instead of explorations, while the widely-adopted SGDs are quite attractive in exploration due to its user-friendly nature and ability in exploring wide optima.

If we manipulate the scheme to propose *an exact swap* in each window instead of *at most one* in the current version, the algorithm shows a better potential in non-convex optimization. In particular, a larger window size corresponds to a slower decay of temperatures in simulated annealing (SAA) (Mangoubi and Vishnoi 2018). Such a mechanism yields a larger hitting probability to move into a sub-level set with lower energies (losses) and a better chance to hit the global optima. Nevertheless, the manipulated algorithm possess the natural of parallelism in cyclical fashions.

Others

Swap time refers to the communication time to conduct a swap in each attempt. For example, chain pair $(p, p + 1)$ of ADJ requires to wait for the completion of chain pairs $(1, 2), (2, 3), \dots, (p - 1, p)$ to attempt the swap and leads to swap time of $O(P)$; however, SEO, DEO, and DEO_{*} don't have this issue because in each iteration, only even or odd chain pairs are attempted to swap, hence the swap time is $O(1)$.

Round trip time refers to the time (stochastic variable) used in a round trip. A round trip is completed when a particle in the p -th chain, where $p \in [P] := \{1, 2, \dots, P\}$, hits the index boundary index at both 1 and P and returns back to its original index p .

Analysis of round trips

The round trip time is hard to analyze due to the non-Markovian index process. To simplify the analysis, we follow [Syed et al. \(2021\)](#) and treat swap indicators as independent Bernoulli variables. Now we make the following assumptions

- (B1) Stationarity: Each sub-process has achieved the stationary distribution $\beta^{(p)} \sim \pi^{(p)}$ for any $p \in [P]$;
- (B2) Weak independence: For any $\tilde{\beta}^{(p)}$ simulated from the p -th chain conditional on $\beta^{(j)}$, $U(\tilde{\beta}^{(j)})$ and $U(\beta^{(j)})$ are independent.

Analysis of round trip time

Proof [Proof of Lemma 1] For $t \in \mathbb{N}$, define $Z_t \in [P] = \{1, 2, \dots, P\}$ as the index of the chain a particle arrives after t windows. Define $\delta_t \in \{1, -1\}$ to indicate the direction of the swap a particle intends to make during the t -th window; i.e., the swap is between Z_t and $Z_t + 1$ if $\delta_t = 1$ and is between Z_t and $Z_t - 1$ if $\delta_t = -1$.

Define $U := \min\{t \geq 0 : Z_t = P, \delta_t = -1\}$ and $V := \min\{t \geq 0 : Z_t = 1, \delta_t = 1\}$. Define $r_p := \mathbb{P}[\text{reject the swap between Chain } p \text{ and Chain } p + 1 \text{ for one time}]$. Define $u_{p,\delta} := \mathbb{E}[U | Z_0 = p, \delta_0 = \delta]$ for $\delta \in \{1, -1\}$ and $v_{p,\delta} := \mathbb{E}[V | Z_0 = p, \delta_0 = \delta]$. Then the expectation of round trip time T is

$$\mathbb{E}[T] = W(u_{1,1} + u_{P,-1}). \quad (16)$$

By the Markov property, for $u_{p,\delta}$, we have

$$u_{p,1} = r_p^W(u_{p,-1} + 1) + (1 - r_p^W)(u_{p+1,1} + 1) \quad (17)$$

$$u_{p,-1} = r_{p-1}^W(u_{p,1} + 1) + (1 - r_{p-1}^W)(u_{p-1,-1} + 1), \quad (18)$$

where r_p^W denotes the rejection probability of a particle in a window of size W at the p -th chain.

According to Eq.(17) and Eq.(18), we have

$$u_{p+1,1} - u_{p,1} = r_p^W(u_{p+1,1} - u_{p,-1}) - 1 \quad (19)$$

$$u_{p,-1} - u_{p-1,-1} = r_{p-1}^W(u_{p,1} - u_{p-1,-1}) + 1. \quad (20)$$

Define $\alpha_p = u_{p,1} - u_{p-1,-1}$. Then by definition, Eq.(19), and Eq.(20), we have

$$\begin{aligned} \alpha_{p+1} - \alpha_p &= (u_{p+1,1} - u_{p,-1}) - (u_{p,1} - u_{p-1,-1}) \\ &= (u_{p+1,1} - u_{p,1}) - (u_{p,-1} - u_{p-1,-1}) \\ &= r_p^W \alpha_{p+1} - r_{p-1}^W \alpha_p - 2, \end{aligned}$$

which implies that

$$a_{p+1} - a_p = -2, \quad (21)$$

for $a_p := (1 - r_{p-1}^W)\alpha_p$. Thus, by Eq.(21), we have

$$a_p = a_2 - 2(p - 2). \quad (22)$$

By definition, $u_{1,-1} = u_{1,1} + 1$. According to Eq.(19), for $p = 1$, we have

$$\begin{aligned} a_2 &= (1 - r_1^W)(u_{2,1} - u_{1,-1}) \\ &= (1 - r_1^W) [u_{1,1} - u_{1,-1} + r_1^W(u_{2,1} - u_{1,-1}) - 1] \\ &= -2(1 - r_1^W) + r_1^W a_2. \end{aligned} \quad (23)$$

Since $r_p \in (0, 1)$ for $1 \leq p \leq P$, Eq.(23) implies $a_2 = -2$ which together with Eq.(22) implies

$$(1 - r_{p-1}^W)\alpha_p = a_p = -2(p - 1), \quad (24)$$

and therefore

$$r_{p-1}^W \alpha_p = -2(p-1) \frac{r_{p-1}^W}{1-r_{p-1}^W}. \quad (25)$$

According to Eq.(20) and Eq.(25), we have

$$u_{P,1} - u_{1,1} = \sum_{p=1}^{P-1} r_p^W (u_{p+1,1} - u_{p,-1}) - (P-1) \quad (26)$$

$$= \sum_{p=1}^{P-1} r_p^W \alpha_{p+1} - (P-1) \quad (27)$$

$$= -2 \sum_{p=1}^{P-1} \frac{r_p^W}{1-r_p^W} p - (P-1). \quad (28)$$

Since $u_{P,1} = 1$, we have

$$\begin{aligned} u_{1,1} &= u_{P,1} + 2 \sum_{p=1}^{P-1} \frac{r_p^W}{1-r_p^W} p + (P-1) \\ &= P + 2 \sum_{p=1}^{P-1} \frac{r_p^W}{1-r_p^W} p. \end{aligned} \quad (29)$$

Similarly, for $v_{p,\delta}$, we also have

$$\begin{aligned} v_{p,1} &= r_p^W (v_{p,-1} + 1) + (1-r_p^W)(v_{p+1,1} + 1) \\ v_{p,-1} &= r_{p-1}^W (v_{p,1} + 1) + (1-r_{p-1}^W)(v_{p-1,-1} + 1). \end{aligned}$$

With the same analysis, we have

$$b_{p+1} - b_p = -2 \quad (30)$$

$$v_{p,-1} - v_{p-1,-1} = r_{p-1}^W (v_{p,1} - v_{p-1,-1}) + 1, \quad (31)$$

where $b_p := (1-r_{p-1}^W)\beta_p$ and $\beta_p := v_{p,1} - v_{p-1,-1}$. According to Eq.(31), we have

$$v_{P,-1} - v_{1,-1} = \sum_{p=1}^{P-1} r_p^W \beta_{p+1} + (P-1). \quad (32)$$

By definition, $v_{P,1} = v_{P,-1} + 1$. According to Eq.(31), for $p = P$, we have

$$\begin{aligned} b_P &= (1-r_{P-1}^W)(v_{P,1} - v_{P-1,-1}) \\ &= (1-r_{P-1}^W) [v_{P,1} - v_{P,-1} + r_{P-1}^W (v_{P,1} - v_{P-1,-1}) + 1] \\ &= r_{P-1}^W b_P + 2(1-r_{P-1}^W). \end{aligned} \quad (33)$$

Since $r_p \in (0, 1)$ for $1 \leq p \leq P$, Eq.(33) implies $b_P = 2$. Then according to Eq.(30), we have

$$b_p = 2(P-p+1),$$

and therefore

$$r_{p-1}^W \beta_p = 2 \frac{r_{p-1}^W}{1-r_{p-1}^W} (P-p+1). \quad (34)$$

By Eq.(32) and Eq.(34), we have

$$v_{P,-1} - v_{1,-1} = 2 \sum_{p=1}^{P-1} \frac{r_p^W}{1-r_p^W} (P-p) + (P-1).$$

Since $v_{1,-1} = 1$, we have

$$v_{P,-1} = 2 \sum_{p=1}^{P-1} \frac{r_p^W}{1-r_p^W} (P-p) + P. \quad (35)$$

According to Eq.(16), Eq.(29) and Eq.(35), we have

$$\mathbb{E}[T] = W(u_{1,1} + u_{P,-1}) = 2WP + 2WP \sum_{p=1}^{P-1} \frac{r_p^W}{1 - r_p^W}.$$

The proof is a generalization of Theorem 1 (Syed et al. 2021); when $W = 1$, the generalized DEO scheme recovers the DEO scheme. For the self-consistency of our analysis, we present it here anyway.

Analysis of optimal window size

Proof [Proof of Theorem 1] By treating $W \geq 1$ as a continuous variable and taking the derivative of $\mathbb{E}[T]$ with respect to W and we can get

$$\begin{aligned} \frac{\partial}{\partial W} \mathbb{E}[T] &= 2P \left[1 + \sum_{p=1}^{P-1} \frac{r_p^W}{(1 - r_p^W)} + W \sum_{p=1}^{P-1} \frac{r_p^W \log r_p}{(1 - r_p^W)^2} \right] \\ &= 2P \left\{ 1 + \sum_{p=1}^{P-1} \frac{r_p^W - r_p^{2W} + W r_p^W \log r_p}{(1 - r_p^W)^2} \right\} \\ &= 2P \left\{ 1 + \sum_{p=1}^{P-1} r_p^W \frac{1 - r_p^W + W \log r_p}{(1 - r_p^W)^2} \right\}. \end{aligned} \quad (36)$$

Assume that $r_p = r \in (0, 1)$ for $1 \leq p \leq P$. Then we have

$$\mathbb{E}[T] = 2WP + 2WP(P-1) \frac{r^W}{1 - r^W}. \quad (37)$$

$$\frac{\partial}{\partial W} \mathbb{E}[T] = \frac{2P}{(1 - r^W)^2} \{ (1 - r^W)^2 + (P-1)r^W(1 - r^W + W \log r) \}. \quad (38)$$

Define $x := r^W \in (0, 1)$. Hence $W = \log_r(x) = \frac{\log x}{\log r}$ and

$$\frac{\partial}{\partial W} \mathbb{E}[T] = f(x) := \frac{2P}{(1-x)^2} \{ (1-x)^2 + (P-1)x(1-x + \log x) \} \quad (39)$$

Thus it suffices to analyze the sign of the function $g(x) := (1-x)^2 + (P-1)x(1-x + \log(x))$ for $x \in (0, 1)$. For $g(x)$, we have

$$g'(x) = (4 - 2P)(x - 1) + (P - 1) \log(x)$$

and

$$g''(x) = 4 - 2P + \frac{P-1}{x}.$$

Thus, $\lim_{x \rightarrow 0^+} g'(x) = -\infty$, $\lim_{x \rightarrow 1} g'(x) = g'(1) = 0$ and $g''(x)$ is monotonically decreasing for $x > 0$.

- For $P > 2$, we know that $g''(x) > 0$ when $0 < x < \frac{P-1}{2(P-2)}$ and $g''(x) < 0$ when $x > \frac{P-1}{2(P-2)}$. Therefore, $g'(x)$ is maximized at $\frac{P-1}{2(P-2)}$.
 - (i) If $P = 3$, by $\log(1+y) < y$ for $y > 0$, we have $g'(x) = 2(\log(1+(x-1)) - (x-1)) < 0$ for any $x \in (0, 1)$. Thus $g(x) > g(1) = 0$ for $x \in (0, 1)$ and therefore $\frac{\partial}{\partial W} \mathbb{E}[T] > 0$ for $W \in \mathbb{N}^+$. $\mathbb{E}[T]$ is globally minimized at $W = 1$.
 - (ii) If $P > 3$, we have the following lemma and the proof is postponed in section .

Lemma 3 (Uniqueness of the solution). *For $P > 3$, there exists a unique solution $x^* \in (0, 1)$ such that $g(x) > 0$ for $\forall x \in (0, x^*)$ and $g(x) < 0$ for $\forall x \in (x^*, 1)$. Moreover, $W^* = \log_r(x^*)$ is the global minimizer for the round trip time.*

- For $P = 2$, we know that $g''(x) > 0$ for $x \in (0, 1)$. Thus $g'(x) < g'(1) = 0$ for $x \in (0, 1)$ and therefore $g(x) > g(1) = 0$ for $x \in (0, 1)$. Then according to Eq.(36), $\frac{\partial}{\partial W} \mathbb{E}[T] > 0$ for $W \in \mathbb{N}^+$. $\mathbb{E}[T]$ is globally minimized at $W = 1$.

In what follows, we proceed to prove that $\frac{1}{P \log P}$ is a good approximation to x^* . In fact, we have

$$\begin{aligned} g\left(\frac{1}{P \log P}\right) &= \left(1 - \frac{1}{P \log P}\right)^2 + \frac{P-1}{P \log P} \left(1 - \frac{1}{P \log P} - \log P - \log(\log P)\right) \\ &= 1 + o\left(\frac{1}{P}\right) - 1 + \frac{1}{\log P} - \frac{\log(\log P)}{\log P} + O\left(\frac{1}{P}\right) \\ &= -\frac{\log(\log P)}{\log P} + O\left(\frac{1}{\log P}\right) \end{aligned}$$

Thus, $\lim_{P \rightarrow \infty} g\left(\frac{1}{P \log P}\right) = 0$.

For $x = \frac{1}{P \log P}$, we have $W = \log_r\left(\frac{1}{P \log P}\right) = \frac{\log P + \log \log P}{-\log r}$. Then according to Eq.(37), for $P \geq 4$,

$$\begin{aligned} \mathbb{E}[T] &= 2P \frac{\log P + \log \log P}{-\log r} \left[1 + (P-1) \frac{\frac{1}{P \log P}}{1 - \frac{1}{P \log P}}\right] \\ &= \left(1 + \frac{1}{\log P} \frac{1}{1 - \frac{1}{P \log P}}\right) \frac{2}{-\log r} (P \log P + P \log \log P) \\ &\leq \left(1 + \frac{1}{\log 4} \frac{1}{1 - \frac{1}{4 \log 4}}\right) \frac{2}{-\log r} (P \log P + P \log \log P) \\ &< \frac{4}{-\log r} (P \log P + P \log \log P) \end{aligned} \tag{40}$$

In conclusion, for $P = 2, 3$, the maximum round trip rate is achieved when the window size $W = 1$. For $P \geq 4$, with the window size $W = \frac{\log P + \log \log P}{-\log r}$, the round trip rate is at least $\Omega\left(\frac{-\log r}{\log P}\right)$.

Remark: Given finite chains with a large rejection rate, the round trip time is only of order $O(P \log P)$ by setting the optimal window size $W \approx \left\lceil \frac{\log P + \log \log P}{-\log r} \right\rceil$. By contrast, the vanilla DEO scheme with a window of size 1 yields a much longer time of $O(P^2)$, where $\frac{1}{-\log(r)} = O\left(\frac{r}{1-r}\right)$ based on Taylor expansion and a large $r \gg 0$.

Technical Lemma Proof [Proof of Lemma 3] To help illustrate the analysis below, we plot the graphs of $g'(x)$ and $g(x)$ for $x \in (0, 1)$ and $P = 5$ in Figure 8. For $P > 3$, since $g'(x)$ is maximized at $x = \frac{P-1}{2(P-2)} \in (0, 1)$ with $g''(x) > 0$ when $0 < x < \frac{P-1}{2(P-2)}$ and $g''(x) < 0$ when $\frac{P-1}{2(P-2)} < x < 1$, $\lim_{x \rightarrow 0^+} g'(x) = -\infty$, and $g'(1) = 0$, we know that $g'\left(\frac{P-1}{2(P-2)}\right) > 0$ and there exists $x_0 \in (0, \frac{P-1}{2(P-2)})$ such that $g'(x) < 0$ (i.e., $g'(x)$ is monotonically decreasing) for any $x \in (0, x_0)$ and $g'(x) > 0$ (i.e., $g'(x)$ is monotonically increasing) for any $x \in (x_0, 1)$. Then $g(x)$ on $(0, 1)$ is globally minimized at $x = x_0$. Moreover, $\lim_{x \rightarrow 0^+} g(x) = 1$ and $g(1) = 0$. Thus, $g(x_0) < g(1) = 0$ and there exists $x^* \in (0, x_0) \subset (0, 1)$ such that $g(x) > 0$ if $x \in (0, x^*)$ and $g(x) < 0$ if $x \in (x^*, 1)$.

Meanwhile, by Eq.(36) and the definition of x , we know that the sign of $\frac{\partial}{\partial W} \mathbb{E}[T]$ is the same with that of $g(x)$ for $W = \log_r(x)$. Thus, $\frac{\partial}{\partial W} \mathbb{E}[T] < 0$ when $W < W^* := \log_r(x^*)$ and $\frac{\partial}{\partial W} \mathbb{E}[T] > 0$ when $W > W^*$, which implies that $\mathbb{E}[T]$ is globally minimized at $W^* = \log_r(x^*)$ with some $x^* \in (0, 1)$.

Discussions on the optimal number of chains in big data

To shed light on the suggestions of the optimal number of chains, we lay out two additional assumptions:

- (B3) Integrability: U^3 is integrable with respect to $\pi^{(1)}$ and $\pi^{(P)}$.
- (B4) Approximate geometric spacing: Assume that $\frac{\tau^{(p+1)}}{\tau^{(p)}} \equiv \left(\frac{\tau^{(P)}}{\tau^{(1)}}\right)^{\frac{1}{P-1}} + o\left(\frac{1}{P}\right)$ for $p \in [P-1]$.

Assumption B3 is a standard assumption in Syed et al. (2021) to establish the convergence of the summation of the rejection rates. Assumption B4 allows extra perturbations to the geometric spacing assumption (Kofke 2002) and is empirically verified in the CIFAR100 example in Figure 7(c).

Proof [Proof of corollary 1] Before we start the proof, we denote by \tilde{r} and \tilde{s} the average rejection and acceptance rates in full-batch settings, respectively. According to section 5.1 in Syed et al. (2021), Assumptions B1, B2 and B3 lead to

$$\tilde{r} = \frac{\Lambda}{P} + O\left(\frac{1}{P^3}\right), \tag{41}$$

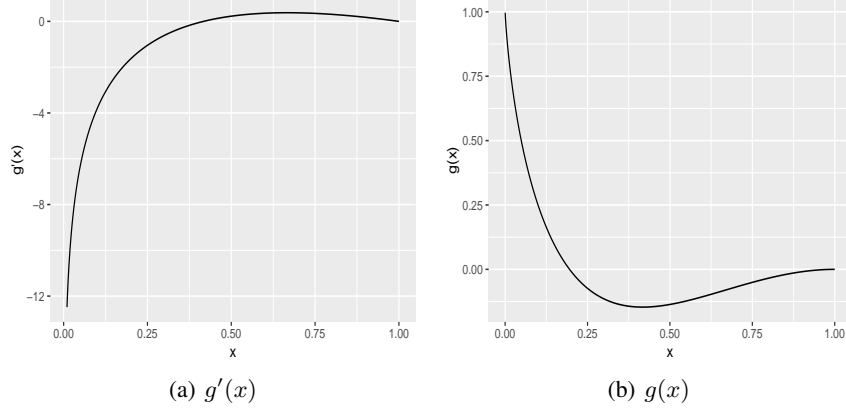


Figure 8: Illustration of functions $g'(x)$ and $g(x)$ for $x \in (0, 1)$ and $P = 5$

where Λ is the barrier, which becomes larger if $\pi^{(1)}$ and $\pi^{(P)}$ have a smaller probability overlap (Predescu, Predescu, and Ciobanu 2004; Syed et al. 2021). Then acceptance rate in full-batch settings is

$$\tilde{s} = 1 - \tilde{r} = 1 - \frac{\Lambda}{P} + O\left(\frac{1}{P^3}\right). \quad (42)$$

By Lemma D4 (Deng et al. 2021) and Eq.(14), a noisy energy estimator with variance $\frac{(\tau^{(p)} - \tau^{(p+1)})^2}{\tau^{(p)^2 \tau^{(p+1)^2}} \sigma_p^2$ yields an average swap rate of $O\left(\tilde{s} \exp\left(-\frac{(\tau^{(p)} - \tau^{(p+1)})^2}{8\tau^{(p)^2 \tau^{(p+1)^2}}\right) \sigma_p^2\right)$. In what follows, the average rejection rate in mini-batch settings becomes

$$r = 1 - O\left(\tilde{s} \exp\left(-\frac{(\tau^{(p)} - \tau^{(p+1)})^2}{8\tau^{(p)^2 \tau^{(p+1)^2}}\right) \sigma_p^2\right), \quad (43)$$

where $p \in [P]$ and more accurate estimates is studied in proposition 2.4 (Gelman, Gilks, and Roberts 1997).

Define $\Delta_\tau = \frac{\tau^{(P)}}{\tau^{(1)}}$. By assumption B4 and Taylor's theorem, we have

$$\left(\frac{\tau^{(p+1)} - \tau^{(p)}}{\tau^{(p)}}\right)^2 := \left(\Delta_\tau^{\frac{1}{P-1}} - 1 + o\left(\frac{1}{P}\right)\right)^2 = \left(\frac{\log \Delta_\tau}{P-1}\right)^2 + o\left(\frac{1}{P^2}\right). \quad (44)$$

Denote $\gamma_p = \frac{\sigma_p}{\tau^{(p+1)}}$. It follows that

$$\begin{aligned} & \exp\left(-\frac{(\tau^{(p)} - \tau^{(p+1)})^2}{8\tau^{(p)^2 \tau^{(p+1)^2}} \sigma_p^2}\right) \\ &= \exp\left(-\left(\frac{(\log \Delta_\tau)^2}{8(P-1)^2} + o\left(\frac{1}{P^2}\right)\right) \frac{\sigma_p^2}{\tau^{(p)^2}}\right) \\ &= \exp\left(-\frac{(\gamma_p \log \Delta_\tau)^2}{8(P-1)^2} + o\left(\frac{1}{P^2}\right)\right). \end{aligned} \quad (45)$$

Plugging it to Eq.(43), we have

$$r = 1 - O\left(\left(1 - \frac{\Lambda}{P} + O\left(\frac{1}{P^3}\right)\right) \exp\left(-\frac{(\gamma_p \log \Delta_\tau)^2}{8(P-1)^2} + o\left(\frac{1}{P^2}\right)\right)\right). \quad (46)$$

Recall in Eq.(40), the round trip time follows that

$$\mathbb{E}[T] = O\left(\frac{P \log P}{-\log r}\right). \quad (47)$$

By $\log(1-t) \leq -t$ for $t \in [0, 1)$ and $\frac{1}{1-t} = 1 + t + O(t^2)$ for a small t , we have

$$\begin{aligned} -\frac{1}{\log r} &= -\frac{1}{\log \left\{ 1 - O \left(\left(1 - \frac{\Lambda}{P} + O \left(\frac{1}{P^3} \right) \right) \exp \left(-\frac{(\gamma_p \log \Delta_\tau)^2}{8(P-1)^2} + o \left(\frac{1}{P^2} \right) \right) \right) \right\}} \\ &\leq \frac{1}{O \left(\left(1 - \frac{\Lambda}{P} + O \left(\frac{1}{P^3} \right) \right) \exp \left(-\frac{(\gamma_p \log \Delta_\tau)^2}{8(P-1)^2} + o \left(\frac{1}{P^2} \right) \right) \right)} \\ &= O \left(\left(1 + \frac{\Lambda}{P} + O \left(\frac{1}{P^3} \right) \right) \exp \left(\frac{(\gamma_p \log \Delta_\tau)^2}{8(P-1)^2} + o \left(\frac{1}{P^2} \right) \right) \right). \end{aligned} \quad (48)$$

Combining Eq.(48) and Eq.(47), we have

$$\begin{aligned} \mathbb{E}[T] &= O \left(P \log P \left(1 + \frac{\Lambda}{P} + O \left(\frac{1}{P^3} \right) \right) \exp \left(\frac{\mu_p^2}{(P-1)^2} + O \left(\frac{1}{P^2} \right) \right) \right) \\ &= O \left(P \log P \exp \left(\frac{\mu_p^2}{P^2} \right) \right), \end{aligned} \quad (49)$$

where $\mu_p := \frac{\gamma_p \log \Delta_\tau}{2\sqrt{2}}$. The optimal P to minimize $\mathbb{E}[T] = O \left(P \log P \exp \left(\frac{\mu_p^2}{P^2} \right) \right)$ is equivalent to the minimizer of $h_p(x) = \log \left\{ x \log x \exp \left(\frac{\mu_p^2}{x^2} \right) \right\} = \log x + \log \log x + \frac{\mu_p^2}{x^2}$ for $x \geq 4$. Then

$$h'_p(x) = \frac{1}{x} + \frac{1}{x \log x} - \frac{2\mu_p^2}{x^3} = \frac{x^2(1 + \frac{1}{\log x}) - 2\mu_p^2}{x^3}, \quad (50)$$

Define $s(x) = x^2(1 + \frac{1}{\log x})$. Then we have

$$s'(x) = 2x + \frac{2x \log x - x}{(\log x)^2} > 0, \quad (51)$$

for $x \geq 4$. Thus $s(x)$ increases with x for $x \geq 4$. Obviously, $\lim_{x \rightarrow \infty} s(x) = \infty$. Since $\mu_p \gg 1$, we know $s(4) < 0$. Thus, there is a single zero point $P_\star \in (4, \infty)$ of $s(x)$ such that $h'_p(x) < 0$ if $x \in [4, P_\star)$ and $h'_p(x) > 0$ if $x > P_\star$. Therefore, $h_p(x)$ is minimized at P_\star with

$$P_\star^2 \left(1 + \frac{1}{\log P_\star} \right) \in \left(2 \min_p \mu_p^2, 2 \max_p \mu_p^2 \right).$$

For any $P_\star \geq 2$, we have $\sqrt{2/(1+1/\log P_\star)} \in (1.1, \sqrt{2})$. Thus, we have the optimal number of chains in mini-batch settings following that

$$P_\star \in \left(1.1 \min_p \mu_p, \sqrt{2} \max_p \mu_p \right) \in \left(\min_p \frac{\sigma_p}{3\tau^{(p+1)}} \log \Delta_\tau, \max_p \frac{\sigma_p}{2\tau^{(p+1)}} \log \Delta_\tau \right). \quad (52)$$

Empirical justification of the optimal number of chains

To obtain an estimate of the optimal number of chains for PT in big data problems, we study the standard deviation of the noisy energy estimators on CIFAR100 via ResNet20 models. We first pre-train a model and then try different learning rates to check the corresponding standard deviation of energy estimators. The reason we abandon the temperature variable is that the widely used data augmentation has drastically affected the estimation of the temperature (Wenzel et al. 2020). Motivated by the linear relation between the learning rate and the temperature in Eq.(5) and the cold posterior affect with the temperature much smaller than 1 (Aitchison 2021), applying Figure 9 and Eq.(52) concludes that P_\star is achieved in an order of thousands in the CIFAR100 example.

The conclusion is different from Syed et al. (2021) since big data problems require a much smaller swap rate to maintain the unbiasedness of the swaps. On the one hand, insufficient chains may lead to insignificant swap rates to generate effective accelerations, but on the other hand, introducing too many chains may be too costly in terms of limited memory and computational budget.

Approximation error for SGD-based exploration kernels

This section proposes to analyze the approximation error when we adopt SGDs as the approximate exploration kernels. Since it is independent of section , different assumptions may be required.

The first subsection shows that for any Gaussian-distributed energy difference estimator $\tilde{U}(\beta^{(p)}) - \tilde{U}(\beta^{(p+1)})$, there exists an optimal \mathbb{C}_\star such that the deterministic swap condition $\tilde{U}(\beta^{(p+1)}) + \mathbb{C}_\star < \tilde{U}(\beta^{(p)})$ perfectly approximates the random event $\tilde{S}(\beta^{(p)}, \beta^{(p+1)}) > u$, where $u \sim \text{Unif}[0, 1]$.

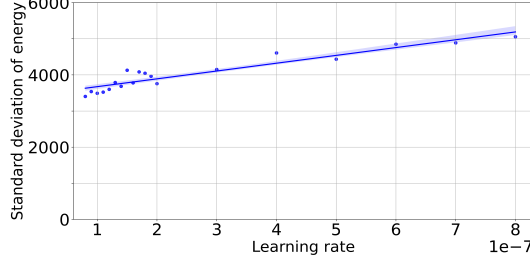


Figure 9: Analysis of standard deviation of energy estimators with respect to different learning rates through ResNet20 on CIFAR100 dataset. Note that we have transformed the average likelihood into the sum of likelihood with a total number of 50,000 datapoints. Hence, the learning rate is also reduced by 50,000 times.

Gap between acceptance rates

To approximate the error when we adopt the *deterministic swap condition* Eq.(7), we first assume the following condition

- (C1) Energy normality: The stochastic energy estimator for each chain follows a normal distribution with a fixed variance.

The above assumption has been widely assumed by [Ceperley and Dewing \(1999\)](#); [Bardenet, Doucet, and Holmes \(2017\)](#); [Seita et al. \(2017\)](#), which can be easily extended to the asymptotic normality assumption depending on large enough batch sizes ([Quiroz et al. 2019](#); [Deng et al. 2021](#)).

Proof [Proof of Lemma 2]

Denote $\partial T_p = \frac{1}{\tau^{(p)}} - \frac{1}{\tau^{(p+1)}} > 0$ for any $p \in [P-1]$, the energy difference $\partial U_p = U(\beta^{(p)}) - U(\beta^{(p+1)})$. By the energy normality assumption C1 and Eq.(14), the energy difference estimator follows that $\partial \tilde{U}_p = \partial U_p(\cdot) + \sqrt{2}\sigma_p \xi$, where $\xi \sim \mathcal{N}(0, 1)$.

Recall from Eq.(15) that the bias-corrected acceptance rate follows that

$$\begin{aligned} \tilde{S}(\beta_t^{(p)}, \beta_t^{(p+1)}) &= 1 \wedge e^{\partial T_p (\tilde{U}(\beta_t^{(p)}) - \tilde{U}(\beta_t^{(p+1)})) - \partial T_p^2 \sigma_p^2} \\ &= 1 \wedge e^{\partial T_p \partial U_p + \sqrt{2} \partial T_p \sigma_p \xi - \partial T_p^2 \sigma_p^2}, \end{aligned} \quad (53)$$

(i) For a uniformly distributed variable $\mu \sim \text{Unif}[0, 1]$, the base swap function satisfies that

$$\begin{aligned} \mathbb{P}\left(\tilde{S}(\beta_t^{(p)}, \beta_t^{(p+1)}) > \mu | \partial U_p\right) &= \int_0^1 \mathbb{P}(\tilde{S}(\beta_t^{(p)}, \beta_t^{(p+1)}) > u | \partial U_p) du \\ &= \int_0^1 \mathbb{P}(e^{\partial T_p \partial U_p + \sqrt{2} \partial T_p \sigma_p \xi - \partial T_p^2 \sigma_p^2} > u | \partial U_p) du \\ &= \int_0^1 \mathbb{P}\left(\xi > \frac{-\partial U_p + \partial T_p \sigma_p^2 + \frac{\log u}{\partial T_p}}{\sqrt{2}\sigma_p}\right) du \end{aligned} \quad (54)$$

(ii) For the deterministic swaps based on Eq.(7), the approximate swap function follows that

$$\mathbb{P}\left(\tilde{U}(\beta_k^{(p+1)}) + \mathbb{C} < \tilde{U}(\beta_k^{(p)}) | \partial U_p\right) = \mathbb{P}(\mathbb{C} < \partial U_p + \sqrt{2}\sigma_p \xi | \partial U_p) = \mathbb{P}\left(\xi > \frac{-\partial U_p + \mathbb{C}}{\sqrt{2}\sigma_p}\right). \quad (55)$$

Denote by $D(u, \mathbb{C}) = \left| \mathbb{P}\left(\xi > \frac{-\partial U_p + \partial T_p \sigma_p^2 + \frac{\log u}{\partial T_p}}{\sqrt{2}\sigma_p}\right) - \mathbb{P}\left(\xi > \frac{-\partial U_p + \mathbb{C}}{\sqrt{2}\sigma_p}\right) \right| \in [0, 2)$. Combining (54) and (55), we

can easily derive that

$$\begin{aligned}
\Delta(\mathbb{C}) &= \mathbb{P}\left(\tilde{S}(\beta_t^{(p)}, \beta_t^{(p+1)}) > \mu | \partial U_p\right) - \mathbb{P}\left(\tilde{U}(\beta_k^{(p+1)}) + \mathbb{C} < \tilde{U}(\beta_k^{(p)}) | \partial U_p\right) \\
&= \int_0^{e^{-\partial T_p^2 \sigma_p^2 + \partial T_p \mathbb{C}}} \underbrace{\mathbb{P}\left(\xi > \frac{-\partial U_p + \partial T_p \sigma_p^2 + \frac{\log u}{\partial T_p}}{\sqrt{2} \sigma_p}\right) - \mathbb{P}\left(\xi > \frac{-\partial U_p + \mathbb{C}}{\sqrt{2} \sigma_p}\right)}_{D(u, \mathbb{C}) \text{ for small enough } u} du \\
&\quad + \int_{e^{-\partial T_p^2 \sigma_p^2 + \partial T_p \mathbb{C}}}^1 \underbrace{\mathbb{P}\left(\xi > \frac{-\partial U_p + \partial T_p \sigma_p^2 + \frac{\log u}{\partial T_p}}{\sqrt{2} \sigma_p}\right) - \mathbb{P}\left(\xi > \frac{-\partial U_p + \mathbb{C}}{\sqrt{2} \sigma_p}\right)}_{-D(u, \mathbb{C}) \text{ for large enough } u} du \\
&= \int_0^{e^{-\partial T_p^2 \sigma_p^2 + \partial T_p \mathbb{C}}} D(u, \mathbb{C}) du - \int_{e^{-\partial T_p^2 \sigma_p^2 + \partial T_p \mathbb{C}}}^1 D(u, \mathbb{C}) du
\end{aligned}$$

Clearly, $\Delta(\mathbb{C})$ is continuous in \mathbb{C} and it is straightforward to verify that

$$\begin{aligned}
\Delta(\partial T_p \sigma_p^2) &= \int_0^{e^{-\partial T_p^2 \sigma_p^2 + \partial T_p^2 \sigma_p^2}} D(u, \partial T_p \sigma_p^2) du - \int_{e^{-\partial T_p^2 \sigma_p^2 + \partial T_p^2 \sigma_p^2}}^1 D(u, \partial T_p \sigma_p^2) du \\
&= \int_0^1 D(u, \partial T_p \sigma_p^2) du \geq 0
\end{aligned}$$

Similarly, $\Delta(-\infty) = -\int_0^1 D(u, \mathbb{C}) du \leq 0$. Moreover, the physical construction suggests that the threshold \mathbb{C} should be strictly positive to avoid radical swap attempts, which implies that there is an optimal solution $\mathbb{C}_\star \in (0, \partial T_p \sigma_p^2]$ that solves $\Delta(\mathbb{C}_\star) = 0$.

Remark 1. Note that the optimal \mathbb{C}_\star may lead to few swaps given a finite number of iterations and sometimes it is suggested to trade in some accuracy to obtain more accelerations (Deng et al. 2020). As such, by setting a desired swap rate via the iterate (12), we can estimate the unknown threshold \mathbb{C} by stochastic approximation (Robbins and Monro 1951). Furthermore, as discussed in Lemma B2 (Deng et al. 2021), the average swap rate follows that $\mathbb{E}[\tilde{S}(\beta_t^{(p)}, \beta_t^{(p+1)})] = O(e^{-\frac{\partial T_p^2 \sigma_p^2}{8}})$. This suggests that for a well-approximated threshold \mathbb{C} , the error is at most $\mathbb{E}[\Delta(\mathbb{C})] = O(e^{-\frac{\partial T_p^2 \sigma_p^2}{8}})$.

Approximate upper bound

The second subsection completes the proof regarding the numerical approximation of SGD-based exploration kernels. Nevertheless, we still require some standard assumptions.

- (C2) Smoothness: The function $U(\cdot)$ is C -smooth if there exists a positive Lipschitz constant C such that $\|\nabla U(x) - \nabla U(y)\|_2 \leq C\|x - y\|_2$ for every $x, y \in \mathbb{R}^d$.
- (C3) Dissipativity: The function $U(\cdot)$ is (a, b) -dissipative if there exist positive constants a and b such that $\langle x, \nabla U(x) \rangle \geq a\|x\|^2 - b$.
- (C4) Gradient normality: The stochastic gradient noise $\varepsilon(\cdot)$ in Eq.(5) follows a Normal distribution $\mathcal{N}(0, \mathcal{M})$ with a fixed positive definite matrix \mathcal{M} .

The assumptions C2 and C3 are standard to show the geometric ergodicity of Langevin diffusion and the diffusion approximations for non-convex functions (Mattingly, Stuart, and Higham 2002; Raginsky, Rakhlin, and Telgarsky 2017; Xu et al. 2018). The assumption C4 is directly motivated by Mandt, Hoffman, and Blei (2017) to track the Ornstein Uhlenbeck (OU) process with a Gaussian invariant measure.

Proof [Proof of Theorem 2] The transition kernel \mathcal{T} of the continuous-time replica exchange Langevin diffusion (reLD) follows that $\mathcal{T} = \prod_p \mathcal{T}^{(p)}$, where each sub-kernel $\mathcal{T}^{(p)}$ draws a candidate $\theta \in \mathbb{R}^d$ with the following probability

$$\mathcal{T}^{(p)}(\theta | \beta^{(p)}, \beta^{(q)}) = (1 - S(\beta_t^{(p)}, \beta_t^{(q)})) Q_p(\theta | \beta^{(p)}) + S(\beta_t^{(p)}, \beta_t^{(q)}) Q_q(\theta | \beta^{(q)}),$$

where $p, q \in \{1, 2, \dots, P\}$, $|p - q| = 1$ and q is selected based on the DEO $_\star$ scheme, $Q_p(\theta | \beta)$ is the proposal distribution in the p -th chain that models the probability to draw the parameter θ via Langevin diffusion conditioned on β , and $S(\beta_t^{(p)}, \beta_t^{(q)})$ follows the swap function in Eq.(2).

Now we consider the following approximations:

$$\text{reLD} \xrightarrow{\text{I}} \text{reSGLD} \xrightarrow{\text{II}} \widehat{\text{DEO}}_{\star}\text{-SGLD} \xrightarrow{\text{III}} \text{DEO}_{\star}\text{-SGLD} \xrightarrow{\text{IV}} \text{DEO}_{\star}\text{-SGD},$$

where $\widehat{\text{DEO}}_{\star}\text{-SGLD}$ resembles the DEO_{\star} scheme except that there are *no restrictions on conducting at most one swap*.

I: Numerical approximation via SGLD By Lemma 1 of (Deng et al. 2020), we know that approximating replica exchange Langevin diffusion via reSGLD yields an error depends on the learning rate and the noise in gradient and energy functions; better results can be obtained by following Theorem 6 of (Sato and Nakagawa 2014) and the details are omitted.

II: Restrictions on at most one swap Adopting at most one swap in the DEO_{\star} scheme includes a stopping time that follows a geometric distribution, which may affect the underlying distribution. Fortunately, the bias can be controlled and becomes smaller in big data problems, which is detailed as follows.

Note that $\widehat{\text{DEO}}_{\star}\text{-SGLD}$ differs from DEO_{\star} in that $\text{DEO}_{\star}\text{-SGLD}$ freezes at most $W - 1$ attempts of swaps in each neighboring chains in each window, while $\widehat{\text{DEO}}_{\star}\text{-SGLD}$ keeps all of these positions open. Recall that the bias-corrected swap rate follows that $\tilde{S} = O(Se^{-O(\sigma^2)})$ by invoking Eq.(15). Following a similar technique in analyzing the bias through the difference of acceptance rates in Lemma 2, we can show that the bias is at most $\tilde{S} - \underbrace{\mathbb{P}(\text{Acceptance rate given frozen swaps})}_{=0} = O(e^{-O(\sigma^2)})$. In other words, the **restrictions on at most one swap**

only lead to a mild bias in big data problems and is less of a concern compared to the local trap problems. Empirically, we have verified the relation between the bias and the variance of noisy energy estimator in a simulated example in section .

III: Deterministic swap condition By Lemma 2 and the mean-value theorem, there exists an optimal correction buffer \mathbb{C}_{\star} to approximate the random event $\tilde{S}(\beta_t^{(p)}, \beta_t^{(p+1)}) > \mu$ through $\tilde{U}(\beta_k^{(p)}) + \mathbb{C}_{\star} < \tilde{U}(\beta_k^{(p+1)})$ in the average sense for any $\beta_t^{(p)}$ and $\beta_t^{(p+1)}$.

IV: Laplace approximation via SGD Assumption C4 guarantees that there exists an optimal learning rate η to conduct Laplace approximation for the target posterior (Mandt, Hoffman, and Blei 2017). Further, by the Bernstein-von Mises Theorem, the approximation error goes to 0 as the number of total data points goes to infinity.

Combining the above approximations, there exists a finite constant $\Delta_{\max} \geq 0$ depending on the learning rates η , the variance of noisy energy estimators, and the choice of correction terms such that the total approximation error of the SGD exploration kernels with *deterministic swap condition* is upper bounded by Δ_{\max} . For any joint probability density μ , the distance between the distributions generated by one step of the exact transition kernel \mathcal{T} and the approximate transition kernel \mathcal{T}_{η} in Eq.(6) is upper bounded by

$$\begin{aligned} & \int_{\beta} d\Omega(\beta) \left| \mu\mathcal{T}(\beta) - \mu\mathcal{T}_{\eta}(\beta) \right| \\ & \leq \int_{\beta} d\Omega(\beta) \left| \int_{\phi, \psi} d\mu(\phi, \psi) \Delta_{\max} \left(Q(\beta|\phi) - Q(\beta|\psi) \right) \right| \\ & \leq \Delta_{\max} \int_{\beta} d\Omega(\beta) \int_{\phi, \psi} d\mu(\phi, \psi) \left(Q(\beta|\phi) + Q(\beta|\psi) \right) \\ & \leq 2\Delta_{\max}, \end{aligned}$$

where $Q(\cdot|\cdot) = \prod_p Q_p(\cdot|\cdot)$. Thus, the one-step total variation distance between the exact kernel and the proposed approximate kernel is upper bounded by

$$\|\mu\mathcal{T}(\beta) - \mu\mathcal{T}_{\eta}(\beta)\|_{\text{TV}} = \frac{1}{2} \int_{\beta} d\Omega(\beta) \left| \mu\mathcal{T}(\beta) - \mu\mathcal{T}_{\eta}(\beta) \right| = \Delta_{\max}. \quad (56)$$

The following is a restatement of Lemma 3 in the supplementary file of Korattikara, Chen, and Welling (2014).

Lemma 4. Consider two transition kernels \mathcal{T} and \mathcal{T}_{η} , which yield stationary distributions π and π_{η} , respectively. If \mathcal{T} follows a contraction such that there is a constant $\rho \in [0, 1)$ for all probability distributions μ :

$$\|\mu\mathcal{T} - \pi\|_{\text{TV}} \leq \rho\|\mu - \pi\|_{\text{TV}},$$

and the uniform upper bound of the one step error between \mathcal{T} and \mathcal{T}_{η} follows that

$$\|\mu\mathcal{T} - \mu\mathcal{T}_{\eta}\|_{\text{TV}} \leq \Delta, \forall \mu,$$

where $\Delta \geq 0$ is a constant. Then the total variation distance between π and π_η is bounded by

$$\|\pi - \pi_\eta\|_{TV} \leq \frac{\Delta}{1 - \rho}.$$

Under the smoothness assumption C2 and the dissipative assumption C3, the geometric ergodicity of the continuous-time replica exchange Langevin diffusion to the invariant measure π has been established (Chen et al. 2019). Combining the exponential convergence of the KL divergence (Deng et al. 2020) and the Pinsker’s inequality (Csiszár and Körner 2011), we have that for any probability density μ , there exists a contraction parameter $\rho \in (0, 1)$ such that

$$\|\mu\mathcal{T} - \pi\|_{TV} \leq \rho\|\mu - \pi\|_{TV},$$

where ρ depends on the spectral gap established in Raginsky, Rakhlin, and Telgarsky (2017) and the swap rate.

Applying Lemma 4, the total variation distance can be upper bounded by

$$\|\pi - \pi_\eta\|_{TV} \leq \frac{\Delta_{\max}}{1 - \rho},$$

which concludes the proof of Theorem 2.

Empirical bias analysis caused by the geometric stopping time

We study the impact of geometric stopping time on the simulations. We try to sample from a Gaussian mixture distribution $e^{-U(x)} \sim 0.4\mathcal{N}(-4, 0.7^2) + 0.6\mathcal{N}(3, 0.5^2)$, where $U(\cdot)$ is the energy function but is not accessible. We can only obtain an energy estimator $\tilde{U}(\cdot) = U(\cdot) + \mathcal{N}(0, \sigma^2)$ in each iteration. We run the two-chain parallel tempering (PT) algorithm based on generalized windows of different sizes. We fix the learning rate 0.01 and set the temperatures as 1 and 10, respectively. The swap condition in the naive case still follows from Eq. (15).

We first try different window sizes ($W = 1, 3, 10, 30, 100, 300, 1000, 3000$) and standard deviations ($\sigma = 3, 4, 5$) for the noisy energy estimators and run the algorithm 5,000,000 iterations. We observe in Figure 10(a), Figure 10(b), and Figure 10(c) that simply running the naive PT algorithm given geometrically-stopped swaps leads to a bias and such a bias becomes larger as we increase the window size. Those swaps tend to overly accept high-temperature samples, which inspires us to include an additional correction term (window-wise) to alleviate the bias (Bardenet, Doucet, and Holmes 2017; Deng et al. 2020) by adopting the window-wise corrected swap rate function in Eq.57. We tune the window-wise correction term λ_W and observe in Figure 10(d), Figure 10(e), and Figure 10(f) that an optimal λ_W exists to significantly reduce the resulting bias caused by the geometric stopping time.

$$a\tilde{S}_W(\beta_{k+1}^{(p)}, \beta_{k+1}^{(p+1)}) = a \cdot \left(1 \wedge e^{\left(\frac{1}{\tau^{(p)}} - \frac{1}{\tau^{(p+1)}}\right) \left(\tilde{U}(\beta_{k+1}^{(p)}) - \tilde{U}(\beta_{k+1}^{(p+1)}) - \left(\frac{1}{\tau^{(p)}} - \frac{1}{\tau^{(p+1)}}\right)\sigma_p^2\right) - \lambda_W} \right). \quad (57)$$

For energy estimators of a larger variance ($\sigma = 6$), we run the naive algorithm more iterations (20,000,000) since the average swap rate is only 0.008% when $W = 1$. However, such a small swap rate also yields a less biased geometrically-stopped swaps as implied in Figure 11(a). We also study the optimal window-wise correction λ_W with respect to the energy variance σ^2 and window size W . We find in Figure 11(b) that λ_W decreases uniformly as we apply a larger σ . This shows a potential to ignore the window-wise correction term λ_W in big data without causing much bias because the variance σ^2 is known to be excessively large (Deng et al. 2020).

We observe in Figure 11(c) that the average swap rate in each window can be significantly improved as we increase the window size. This is a promising alternative to improve the swap rate via generalized windows compared to including sufficiently many chains (Syed et al. 2021). For example, given $\sigma = 6$, the corrected swap rate blows up from 0.008% given $W = 1$ to 11.1% when $W = 3000$, which is a 1,400 times of increase of swap rates, although the number of windows is also reduced by 3,000 times. Recall that the round trip time has a quadratic dependence on the swap rate r when r is not close to 1 (see Theorem 1 in (Syed et al. 2021)). **The empirical study shows a potential to approximately reduce the round trip time by a thousand (1400²/3000) times!** The generalized windows seem to have an averaging ability to reduce the variance of the noisy energy estimators and the improvement is more significant as we apply a larger variance σ^2 .

For future works, we are interested in studying how to theoretically derive the window-wise correction λ_W and understand more on the dependence of λ_W with respect to σ and W . We are also interested in obtaining a good estimate of λ_W efficiently via stochastic approximation.

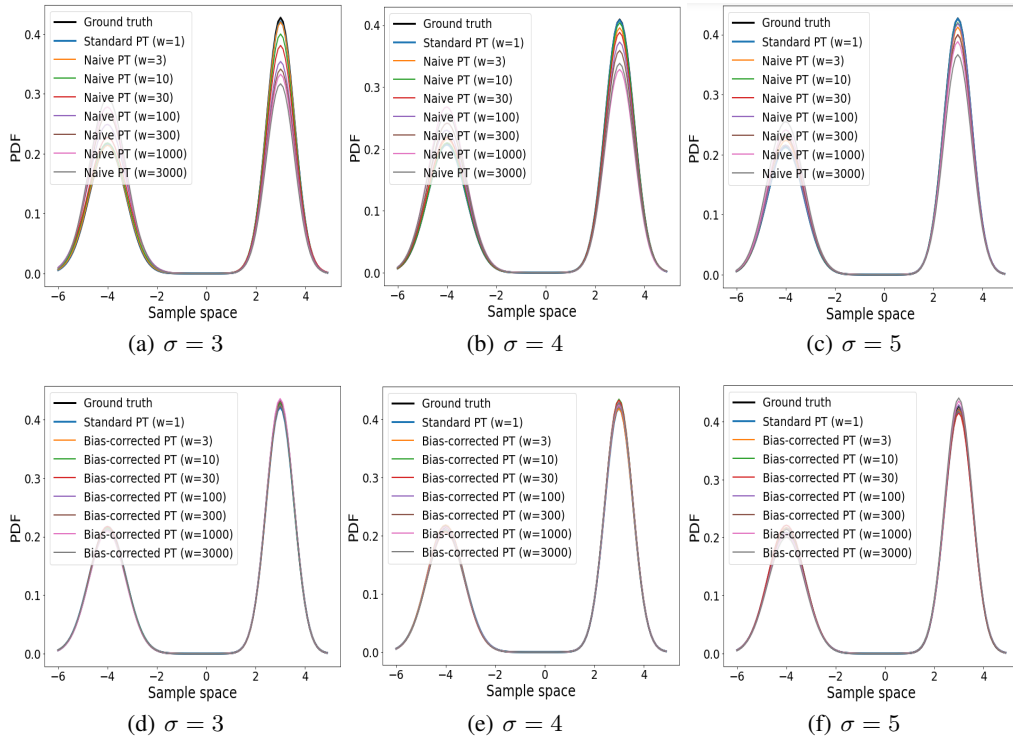


Figure 10: Simulations of a Gaussian mixture distribution based on different window size W and energy variance σ^2 .

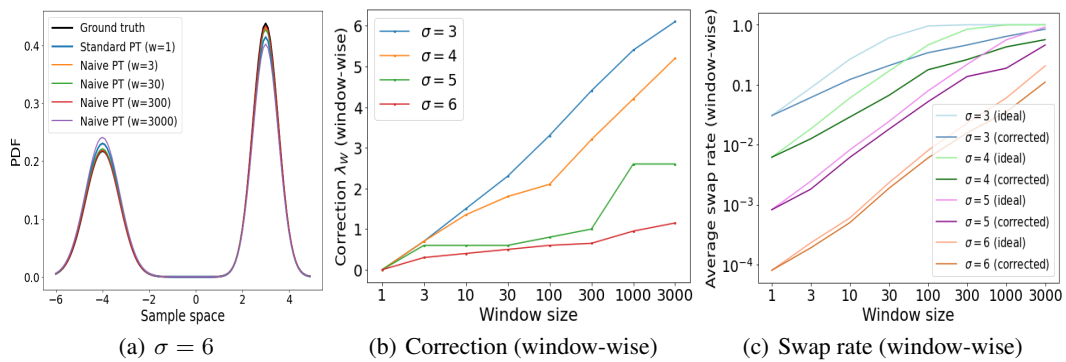


Figure 11: Relations between key criteria. In subfigure (b), the ideal swap rate means no correction is applied such that the rate goes to 1 geometrically fast as the window size increases.